THE EXPERIMENTAL DETERMINATION AND ANALYTICAL VERIFICATION OF THE AGE OF PU-BE SOURCE NEUTRONS IN GRAPHITE

by

CHARLES URBAN STEICHEN

B. S., Kansas State University, 1959

A THESIS

submitted in partial fulfillment of the

requirements for the degree

MASTER OF SCIENCE

Department of Nuclear Engineering

KANSAS STATE UNIVERSITY
OF AGRICULTURE AND APPLIED SCIENCE

1960

TABLE OF CONTENTS

INTRODUCTION

The properties and constants associated with neutron sources are important quantities in the study of the behavior of neutrons in various materials. In particular, in the study of neutron diffusion in sub-critical reactor assemblies, it is important to know the properties associated with the slowing down of the source neutrons in the moderating material.

In recent years, Pu-Be neutron sources have become widely used as the source of neutrons for the study of neutron behavior in sub-critical reactor assemblies. The popularity of the Pu-Be sources is due to the long half life of the sources, the relatively small amount of associated gamma-ray activity and the relative ease of preparation of uniform sources.

Because of future plans to study the diffusion of neutrons from a Pu-Be source in the Kansas State University graphite sub-critical assembly and the unavailability of the required value of the age for this source in graphite, a series of experiments was undertaken to determine the age of Pu-Be source neutrons in graphite and theoretical calculations were performed to predict the age from the calculated and measured source energy spectra.

In these experiments, the age was determined by measuring the spatial distribution of the slowing down density at the 1.44 ev resonance of indium.

The theoretical value of the age was obtained by calculating the age of the neutrons from source spectrum energies to fission

spectrum energies and then adding to this the accepted value of the age from the fission spectrum to 1.44 ev. The calculated portion of the total age to 1.44 ev was obtained by using the expression for the age as defined by the Fermi continuous slowing down model and the existing source energy spectra and cross sections.

LITERATURE SURVEY

To the author's knowledge, there was no published literature available on the age of Pu-Be neutrons in graphite. However, numerous publications were available describing techniques for measuring the age experimentally, and a limited number of references were available concerning age measurements, in graphite, for sources whose energy spectra is similar to that of Pu-Be, i.e., Po-Be and Ra-α-Be.

The combined works of Marshak (14), Weinberg and Wigner (19) and Amaldi (1), give a rather complete review of the theoretical background and developments, concerning the problem of neutron slowing down. These works also review experimental techniques for making age measurements and discuss some of the methods used to calculate slowing down distributions and age.

Hill, Roberts and McCammon (9), have measured the age, to indium resonance, of fission neutrons in graphite and discuss the effects of foil spacing, cadmium thickness and foil activities induced by other than resonance neutrons. They give an

interesting discussion of the transport correction for the finite thickness of the indium foils.

A derivation of an approximate equation to correct for the finite sizes of sources and foils, used in age measurements, is given by Hill, Roberts and Fitch (8), as used in their experimental determination of the age of fission neutrons in light water.

Wade (18), in his studies of the slowing down distribution of neutrons in light and heavy water mixtures, gives an indium self-shielding method for determining the amount of foil activity induced in cadmium covered indium foils by other than resonance neutrons.

An estimation of the required size of the measuring column, for age measurements in graphite, for an error of less than one per cent in the measured age, is given by Davis (4) in his study of a slowing down experiment.

Hughes (12) has reported the experimental age of Ra-α-Be neutrons in graphite and Bogart, Cusick and Shook (2) have reported the experimental ages of Ra-α-Be and Po-Be neutron ages in graphite. Hughes also reported an experimental fit for the slowing down distribution from a standard Ra-α-Be source in the Argonne National Laboratory standard graphite pile.

Few results are available for the calculation of neutron ages in graphite. The more rigorous methods of calculation involve the method of moments or Monte Carlo methods, using high

speed digital computers. Bogart, Cusick and Shook, have also reported the calculated ages, in graphite, of Po-Be, Ra-α-Be and fission neutrons, using the Monte Carlo technique developed at the Oak Ridge National Laboratory.

Faulkner (5) has reported a method of calculating fission neutron ages in heavy moderators, using the Fermi age theory and the analytical expression for the fission neutron spectrum. The expression for the age was derived stressing the importance of the analytical expression for the fission spectrum and assumed average values for the neutron cross sections over large sections of the energy range.

The neutron energy spectrum for a Pu-Be source has been measured experimentally by Stewart (16) and has been calculated by Hess (10).

THEORY

Experimental

The slowing down density, in an infinite medium, from a point source, as given by the Fermi age theory, is (6)

$$q(r,\tau) = \frac{e^{-r^2/4\tau}}{(4\pi\tau)^{3/2}} \qquad (1)$$

where τ is the Fermi age, in cm^2, of the neutrons of source energy E_o, to a given energy E, and r is the distance from the source to the point of interest. The slowing down density,

$q(r,\tau)$, can be defined as the number of neutrons/cm^2-sec which slow down past a given energy E, corresponding to the age τ, at a given point r.

To obtain a physical significance of the age, the second moment of the slowing down density, denoted by $\overline{r^2}$, can be considered. The second moment is given as

$$\overline{r^2} = \frac{\int_V r^2 q(r,\tau)\, dV}{\int_V q(r,\tau)\, dV} \tag{2}$$

For a point source, in an infinite medium, this expression becomes

$$\overline{r^2} = \frac{\int_0^\infty r^2 [4\pi r^2 q(r,\tau)]\, dr}{\int_0^\infty 4\pi r^2 q(r,\tau)\, dr} \tag{3}$$

Substituting Eq. (1) into this equation for $q(r,\tau)$ and performing the indicated integration

$$\overline{r^2} = \frac{\int_0^\infty r^4 e^{-r^2/4\tau}\, dr}{\int_0^\infty r^2 e^{-r^2/4\tau}\, dr} = 6\tau \tag{4}$$

Therefore, the age, τ, can be seen to be one-sixth of the mean square (crow flight) distance traveled by a neutron from age zero, to the time at which its age is τ.

Experimentally we measure the activation, A, of a foil which is proportional to

$$\int \phi(E)\Sigma(E)dE \qquad (5)$$

where $\phi(E)$ is the flux of neutrons of energy E, and $\Sigma(E)$ is the macroscopic activation cross section of the foil for neutrons of energy E. It has been shown (9) that the activity of indium foils, covered with a sufficient thickness of cadmium, is essentially due only to the activation caused by neutrons in the 1.44 ev resonance range. Therefore, to a first approximation, the slowing down density, q, can be taken as being proportional to the cadmium covered indium foil activity, and the expression for the age then becomes

$$\tau(\text{source} \rightarrow 1.44\text{ev}) = \frac{\int_0^\infty A(r) r^4 dr}{6\int_0^\infty A(r) r^2 dr} \qquad (6)$$

The distribution given by Eq. (1) does not correspond exactly to the actual measured distribution. The derivation of Eq. (1) is based on the Fermi age equation and is, therefore, subject to the assumptions made in deriving this equation. These assumptions are as follows:

1) The energy loss is a continuous function. This means that the average number of slowing down collisions must be large so that the average energy loss per collision is small. This assumption is therefore good for heavy moderators.

2) No absorption during the slowing down process.

3) Small distance from source.

4) Fractional rate of change of mean free path in one collision interval is small.

In addition to these assumptions, Eq. (1) is derived using a monoenergetic source of neutrons. For a polyenergetic source of neutrons, the distribution given by the Fermi age theory would be a summation of a series of terms such as given by Eq. (1).

Even if the distribution is not Gaussian, the relation between τ and $\overline{r^2}$, given by Eq. (4), still holds (19). However, in that case, $\sqrt{\tau}$ is more properly called the "slowing down length."

In order to perform the integrations, from 0 to ∞, as indicated by Eq. (6), it is necessary to study the behavior of the distribution at large distances from the source. As seen from the third assumption, used in deriving the Fermi age equation, the distribution as given by Eq. (1) is not valid at large distances from the source. Physically it is to be expected that most neutrons, at great distances from the source, arrive at these distances after a large number of small angle collisions, each associated with a small energy loss. Therefore, an upper bound on the resonance neutron density at large r can be obtained by assuming that the neutrons which reach large r all travel in a straight line. These neutrons, after finally colliding, will be moderated without moving very far (relative to the distance already traveled) from the point of collision. The number of

such neutrons that have not suffered a collision, and the resonance energy neutrons resulting from them, will decrease with distance from the source r and will be proportional to

$$\frac{e^{-r/\lambda}}{r^2}$$

This is a simple exponential decrease, combined with an inverse characteristic of a point source. At large r, the principal variation in the slowing down density arises from the exponential and the change in slowing down density is less rapid than that given by the Gaussian of Eq. (1). Using this exponential character of the distribution, the integrals in Eq. (6) can be integrated from the last data point to ∞.

In the discussion so far, the sources and detectors have been assumed to be point sources and point detectors and the measured activity has been assumed to be proportional to the slowing down density. In general, the source and detector geometries and the measured activity is not strictly proportional to the slowing down density at 1.44 ev. The correction for the geometry is given in the Appendix.

Analytical

The energy of the neutrons from a Pu-Be source, are considerably greater (16) than those from a fission source, and as the cross sections are functions of energy, the age of the Pu-Be neutrons will also differ considerably from the age of fission neutrons.

As the experimental value for the age of fission neutrons is a well known quantity, it seems plausible that a reasonably good value for the age of Pu-Be neutrons could be obtained by calculating the age of the Pu-Be source neutrons from source energies to fission energies and then adding to this value the age of fission neutrons from the fission spectrum energies to the indium resonance energy of 1.44 ev; or to thermal energies, by adding the additional value of the age from indium resonance to thermal. By using this procedure, a relatively large error, in the calculations of the age from the source spectrum energy, should still result in a small error in the final result, as the value of the age from the fission spectrum to indium resonance is much larger than the value from the source spectrum to the fission spectrum.

Assuming the Fermi age theory to be a good approximation for the age in graphite, the age from source energies to fission energy can be determined from the expression defining the age, τ, in the Fermi age theory. This expression is given as (6)

$$\tau(E_o, E) \equiv \int_E^{E_o} \frac{D(E)}{\xi \Sigma_s(E)} \frac{dE}{E} \qquad (7)$$

where E_o is the source energy, E is the energy to which τ is to be measured, ξ is the average logarithmic energy decrement per collision, D is the diffusion coefficient, and Σs is the macroscopic scattering cross section. This equation can also be written as

$$\tau(E_o, E) = \frac{1}{3(1-\bar{\mu}_o)\xi} \int_E^{E_o} \frac{1}{\Sigma_s^2(E)} \frac{dE}{E} \tag{8}$$

where $$D \doteq \frac{1}{3\Sigma_s(1-\bar{\mu}_o)}$$

and $\bar{\mu}_o$, the average cosine of the scattering angle in the laboratory system, can be written as (6)

$$\bar{\mu}_o = \frac{2}{3A}$$

for slightly absorbing media.

By assuming the cross sections to be linear functions of energy between small increments of energy, E_n' to $(E_o')_n$, the expression for τ can be rewritten as

$$\tau(E_o, E) = \frac{1}{3(1-\bar{\mu}_o)\xi} \int_{E_m'}^{(E_o')_m} \frac{1}{\Sigma_s^2(E)} \frac{dE}{E} \tag{9}$$

where $$\Sigma_s(E) = mE + \Sigma_o$$

the equation of a straight line with slope m and intercept Σ_o, and

$$K = \frac{1}{3(1-\bar{\mu}_o)\xi}$$

Writing Σ_s in terms of σ_s, the microscopic scattering cross section, Eq. (9) becomes

$$\tau(E_o,E) = K' \int_{E_m'}^{(E_o')_m} \frac{1}{\sigma_s^2(E)} \frac{dE}{E} \tag{10}$$

where $\sigma_s(E) = mE + \sigma_o$

$$K' = \frac{A^2}{3\rho^2 N_A^2 (1-\bar{\mu}_o)\xi}$$

and A = atomic weight of moderator

ρ = density of moderator

N_A = Avogadro's number.

The integral in Eq. (10) is of standard form

$$y(x) = \int_a^b \frac{dx}{x(ax+b)^2}$$

the solution of which can be obtained from a table of integrals.

Performing the integration, Eq. (10) becomes

$$\tau(E_o,E) = K'\left[\frac{1}{\sigma_o^2} \ln\left|\frac{(E_o')_m (mE_m'+\sigma_o)}{E_m' [m(E_o')_m+\sigma_o]}\right| + \frac{1}{\sigma_o}\left(\frac{1}{m(E_o')_m+\sigma_o} - \frac{1}{mE_m'+\sigma_o}\right)\right] \tag{11}$$

$$= K'\left[\frac{1}{\sigma_o^2} \ln\left|\frac{(E_o')_m \sigma(E_m')}{E_m' \sigma(E_o')_m}\right| + \frac{1}{\sigma_o}\left(\frac{1}{\sigma(E_o')_m} - \frac{1}{\sigma(E_m')}\right)\right] \tag{12}$$

For the case where $\sigma_o = 0$, Eq. (10) reduces to

$$\tau(E_o,E) = K' \int_{E_m'}^{(E_o')_m} \frac{1}{(mE)^2} \frac{dE}{E} \tag{13}$$

The integration of this expression is straightforward and upon integration the expression becomes

$$\tau(E_o,E) = \frac{K'}{2m^2} \left[\frac{1}{(E_m')^2} - \frac{1}{(E_o')_m^2} \right] \tag{14}$$

For a neutron source emitting neutrons of several different energies, the slowing down density, as given by the Fermi age theory, from a point source in an infinite medium, can be written as a summation of the infinite slowing down kernels, as given in Eq. (1), where each kernel is multiplied by a fraction representing the fraction of neutrons with energy corresponding to the value of τ used in that particular kernel.

The expression for the slowing down density from a polyenergetic source then becomes

$$q(r,\tau) = Q \sum_{i=1}^{n} f_i(E) \frac{e^{-r^2/4\tau_i}}{(4\pi\tau_i)^{3/2}} \tag{15}$$

where $f_i(E)$ is the fraction of source neutrons with energy E and Q is the total source strength.

Substituting Eq. (15) into the expression for the second moment of the slowing down distribution, given by Eq. (6), and using the definition, $\tau = \frac{\overline{r^2}}{6}$, the expression for the age of the polyenergetic source can be written as

$$\tau = \frac{\overline{r^2}}{6} = \frac{Q\int_0^\infty 4\pi r^4 \sum_{i=1}^{n} f_i \frac{e^{-r^2/4\tau_i}}{(4\pi\tau_i)^{3/2}} dr}{6Q\int_0^\infty 4\pi r^2 \sum_{i=1}^{n} f_i \frac{e^{-r^2/4\tau_i}}{(4\pi\tau_i)^{3/2}} dr} \tag{16}$$

$$= \frac{\sum_{i=1}^{n} f_i \int_0^\infty r^4 \frac{e^{-r^2/4\tau_i}}{(4\pi\tau_i)^{3/2}} dr}{6\sum_{i=1}^{n} f_i \int_0^\infty r^2 \frac{e^{-r^2/4\tau_i}}{(4\pi\tau_i)^{3/2}} dr} \tag{17}$$

The solutions of the integrals in Eq. (17) are of the form

$$\int_0^\infty x^{2m} e^{-ax^2} dx = \frac{1\cdot 3\cdot 5\cdots(2m-1)}{2^{m+1} a^m}\sqrt{\frac{\pi}{a}} \tag{18}$$

Performing the integrations, Eq. (17) becomes

$$\tau(E_o, E) = \frac{\overline{r^2}}{6} = \frac{\sum_{i=1}^{n} f_i \tau_i}{\sum_{i=1}^{n} f_i} \tag{19}$$

For $\sum_{i=1}^{n} f_i = 1$, Eq. (19) reduces to

$$\tau(E_o, E) = \sum_{i=1}^{n} f_i \tau_i \tag{20}$$

Therefore, the age from any source spectrum to a fission spectrum, or to some lower energy, can be approximated by taking a small incremental fraction, $f_i(E)$, of neutrons and calculating the age for this fraction of the neutrons between the average energies of this fraction in the source and fission spectrum, multiplying by the fraction and summing over all neutrons. Eq. (10) can then be written

$$\tau(E_o,E) = K' \sum_{i=1}^{m} f_i \int_{\bar{E}_i}^{(\bar{E}_o)_i} \frac{1}{\sigma_s^2(E)} \frac{dE}{E} \tag{21}$$

when $$\sum_{i=1}^{m} f_i = 1$$

Eq. (21) can also be written as

$$\tau(E_o,E) = K' \sum_{i=1}^{j} f_i \left[\int_{\bar{E}_i}^{E_1'} \frac{1}{\sigma_s^2(E)} \frac{dE}{E} + \int_{E_2'}^{E_3'} \frac{1}{\sigma_s^2(E)} \frac{dE}{E} + \cdots \int_{E_m'}^{(\bar{E}_o)_i} \frac{1}{\sigma_s^2(E)} \frac{dE}{E} \right] \tag{22}$$

where $\bar{E}_i \leqq E_n' \leqq (\bar{E}_o)_i$.

As the cross sections are all assumed to be linear functions of energy between E_n' and E_{n+1}', the summation of integrals in Eq. (22) can be replaced by a summation of solutions given by Eq.'s (12) or (14), depending upon σ_o being equal to or greater than zero.

Again, as pointed out in the earlier discussion on the experimental determination of age, the slowing down distribution as given by the age theory, does not correspond exactly to the actual slowing down distribution. The age approximation and the Gaussian slowing down distribution which it yields, as derived from the Boltzman equation, resulted from a spherical harmonic expansion of the angular distribution and a Taylor's series expansion of the energy distribution of the neutrons. The Taylor's series expansion is valid only if the mean free path varies slowly over one slowing down interval, while the spherical harmonic expansion could be expected to be good fairly near the source. Thus, the age approximation is poor where the mean free path changes rapidly or at large distances from the source in any medium.

The failure of the age theory to describe the slowing down distribution, at large distances from the source, is well described by considering the following argument (19). Neutrons which have made no collisions at all will be distributed according to

$$q = \frac{Q \Sigma_s(E_0) e^{-\Sigma_s(E_0) r}}{4\pi r^2} \qquad (23)$$

where Σ_s is the macroscopic scattering cross section and Q is the source strength. At small distances, the Gaussian slowing down distribution will exceed this exponential, but at large distances, the ratio

$$\frac{\text{source neutrons}}{\text{Gaussian moderated neutrons}} = \left(\frac{\Sigma_s e^{-\Sigma_s r}}{4\pi r^2}\right)\left(\frac{(4\pi\tau)^{3/2}}{e^{-r^2/4\tau}}\right)$$

approaches infinity, since the Gaussian falls off faster than the exponential. Therefore, at large distances, the distribution is more exponential than Gaussian.

An improvement on the age theory distribution can be expected if the "aging" process, which leads to the Gaussian, is assumed to begin only after the neutrons have made their first collisions (19). The points at which first collisions occur act as "sources" for the slowing down process.

The first collisions are distributed as given in Eq. (23) and accordingly the slowing down distribution should be

$$q(r,\tau) = \int_0^\infty \frac{\Sigma_s(E_0) e^{-\Sigma_s(E_0)|r'|}}{4\pi r'^2} \frac{e^{-|r'-r|^2/4\tau}}{(4\pi\tau)^{3/2}} dr' \qquad (24)$$

where r' represents the point of first collision.

A further improvement can be made by taking into account the fact that after a neutron has suffered a collision which throws it across energy E, it experiences a "free ride," without changing its energy, until it suffers its next collision. To take this into account, it is plausible to include another exponential with mean free path appropriate to the lower energy. Thus, the slowing down distribution, including first and last collisions, is

$$q(r,\tau) = \int_0^\infty \int_0^\infty \frac{\Sigma_s(E_0)\, e^{-\Sigma_s(E_0)|r'|}}{4\pi r'^2} \frac{e^{-|r''-r'|^2/4\tau}}{(4\pi\tau)^{3/2}} \frac{e^{-\Sigma_s(E)|r''-r|}}{4\pi|r''-r'|} dr'dr'' \qquad (25)$$

This equation can be thought of as being a convolution of three separate kernels and the second moment of a distribution which is the convolution of several kernels is the sum of the second moments of each kernel (19). Applying this to the distribution given in Eq. (25), the second moment of the slowing down distribution, corrected for first and last collisions, is given as

$$\overline{r^2} = \frac{2}{\Sigma_s^2(E_0)} + 6\tau + \frac{2}{\Sigma_s^2(E)} \qquad (26)$$

This result can also be obtained by observing that $\overline{r^2}$ is the mean square distance a neutron travels in slowing down from energy E_0 to E. To obtain the overall $\overline{r^2}$ for the distribution, the mean square distance the neutron travels to reach its first collision point and the mean square distance the neutron travels in its free ride after its last collision, must be added to the mean square distance obtained from the distribution given by the Fermi age theory. The total mean square distance traveled is then

$$\overline{r^2} = \overline{r_1^2}\ (\text{first collision}) + 6\tau + \overline{r_2^2}\ (\text{last collision}) \qquad (27)$$

$$= \frac{\int_0^\infty r^2 \Sigma_s(E_0)\, e^{-\Sigma_s(E_0) r}\, dr}{\int_0^\infty \Sigma_s(E_0)\, e^{-\Sigma_s(E_0) r}\, dr} + 6\tau + \frac{\int_0^\infty r^2 \Sigma_s(E)\, e^{-\Sigma_s(E) r}\, dr}{\int_0^\infty \Sigma_s(E)\, e^{-\Sigma_s(E) r}\, dr} \qquad (28)$$

$$= \frac{2}{\Sigma_s^2(E_0)} + 6\tau + \frac{2}{\Sigma_s^2(E)} \qquad (29)$$

which is the same as the result obtained before.

The distribution given by Eq. (26) is difficult to handle analytically and it is, therefore, customary to replace it by the single Gaussian as given by Eq. (1), when τ is replaced by the corrected age, which is chosen to give the same second moment as Eq. (27). Thus, the corrected age is

$$\tau = \frac{\overline{r^2}}{6} = \frac{1}{3\Sigma_s^2(E_0)} + \int_E^{E_0} \frac{D}{\xi \Sigma_s(E)} \frac{dE}{E} + \frac{1}{3\Sigma_s^2(E)} \qquad (30)$$

As the first collision effect is already taken into account in the experimental fission neutron age, the portion of the effect included in the fission age, should be subtracted from the age obtained between the source energies of interest to the fission energy. The first collision correction then becomes

$$\text{First Collision Correction} = \frac{1}{3}\left(\frac{1}{\Sigma_s^2(E_o)} - \frac{1}{\Sigma_s^2(E)}\right) \quad (31)$$

The last collision effect is also already included in the experimental fission age and, therefore, this correction is zero when using the method of calculation described in this paper.

Rewriting Eq. (22), the expression for τ, including the corrections, becomes

$$\tau(E_o,E) = \sum_{i=1}^{j} f_i \left[K'' \left(\frac{1}{\sigma_s^2(E_o)} - \frac{1}{\sigma_s^2(E)}\right) + K' \left(\int_{\bar{E}_i}^{E_1} \frac{1}{\sigma_s^2(E)} \frac{dE}{E} + \int_{E_2'}^{E_3'} \frac{1}{\sigma_s^2(E)} \frac{dE}{E} + \cdots \int_{E_m'}^{(\bar{E}_o)_i} \frac{1}{\sigma_s^2(E)} \frac{dE}{E} \right) \right] \quad (32)$$

EXPERIMENTAL

Apparatus

The graphite column, shown in Plate I, in which the measurements were made, consisted of a rectangular parallelepiped, 68 inches square and 100 inches high, resting on a concrete foundation. The column was constructed by stacking layers of machined reactor grade graphite blocks, approximately 4 inches in cross section and of various lengths. In stacking, the long dimension of the graphite blocks was alternated by 90° from layer to layer.

EXPLANATION OF PLATE I

Photograph of graphite measuring column

PLATE I

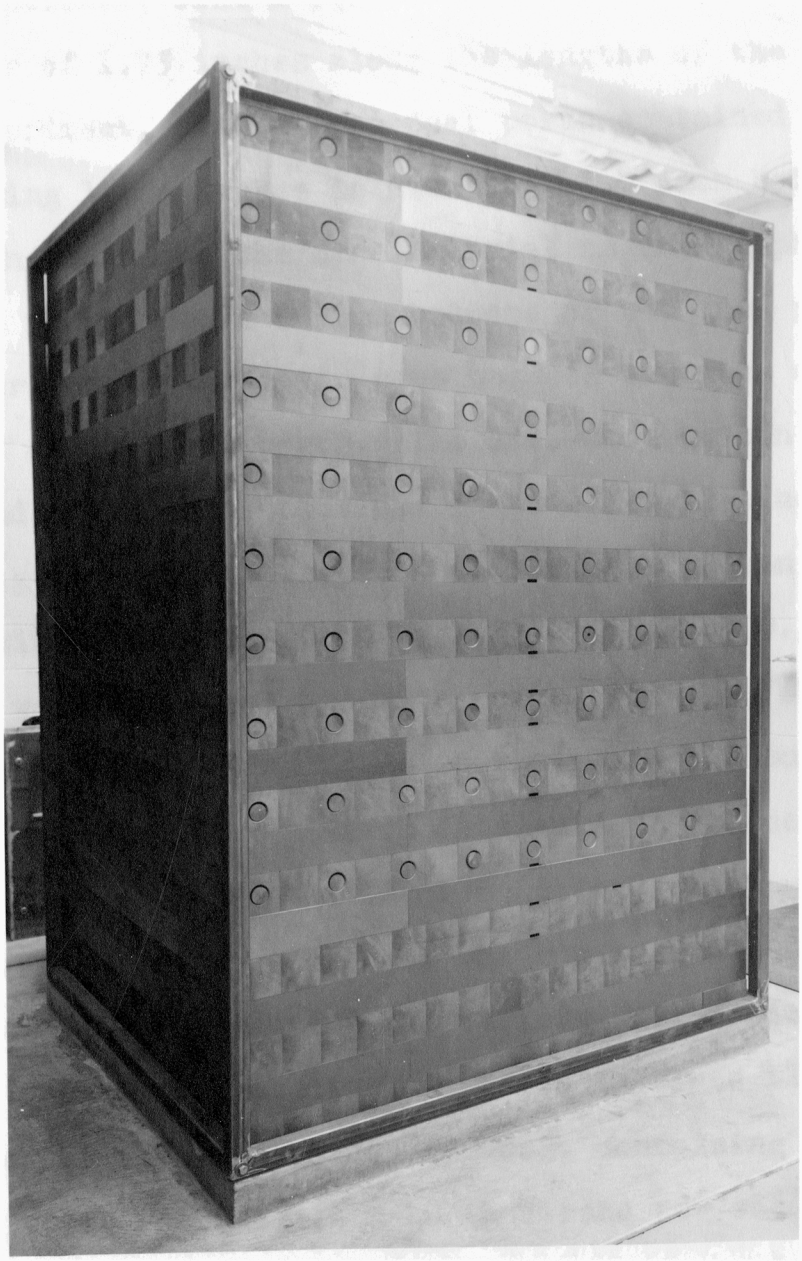

As seen in Plate I, certain of the graphite blocks, in a given geometrical pattern, with a square pitch of 8 inches, were drilled to a diameter of 1.75 inches along the lengths of the blocks. For this experiment, each of the fuel ports contained graphite plugs measuring 1.625 inches in diameter with each being 22.68 inches in length and of the same material as the graphite blocks. The graphite plugs rested on the bottoms of the fuel ports and there were crescent shaped air gaps between the tops of the plugs and the tops of the fuel ports. The distance between the tops of the plugs and the tops of the fuel ports was 0.125 inches. The blocks, along the central vertical axis of the column, contained foil slots with a cross section of 1.281 inches by 0.343 inches. These slots were such that graphite foil stringers, shown in Plate II, containing indium foils in their cadmium boxes, could be placed at approximately 4-inch intervals up the central axis of the column, except for the first position, which was approximately 2 inches from the center of the source. A schematic diagram of the column, showing the various foil positions in relation to the source location, is given in Plate III.

The one curie Pu-Be neutron sources, containing 16 grams of Pu, emitted approximately 1.4×10^6 neutrons per second. The sources were constructed such that the source material was held in an inner container of titanium and in an outer container of stainless steel, 1.02 inches in diameter and 1.30 inches long.

The sources were held in individual graphite positioning cylinders, shown in Plate II, of inner diameter such that the

EXPLANATION OF PLATE II

Photograph of the graphite foil stringer and graphite source positioning cylinder

Legend:

A. Graphite source positioning cylinder

B. Graphite foil stringer, showing a cadmium box in position in the center depression

PLATE II

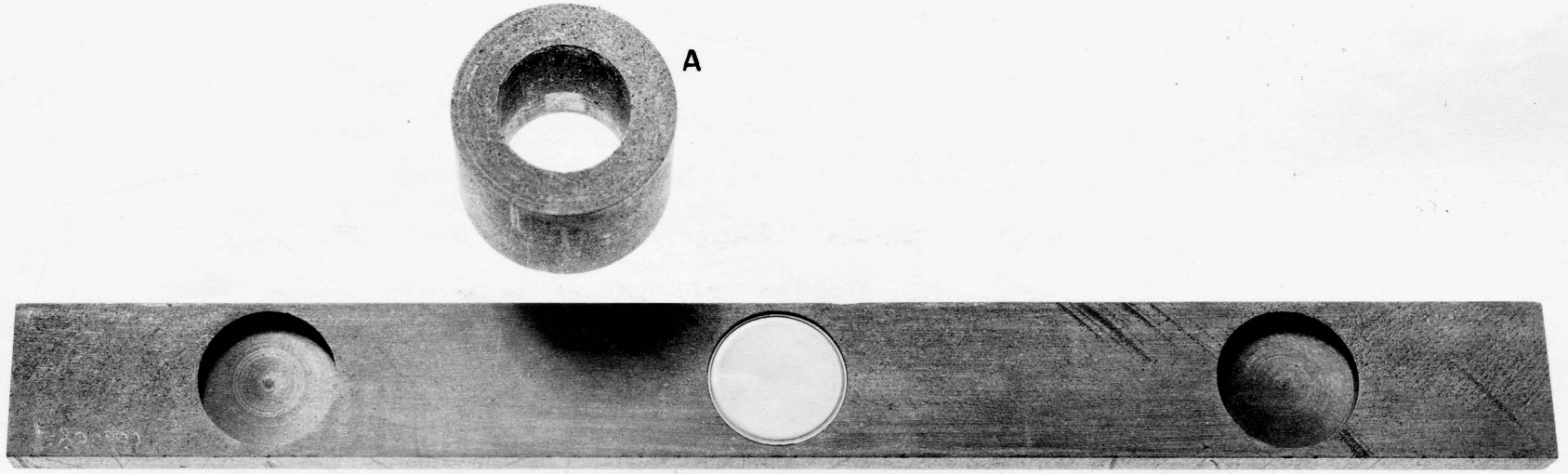

EXPLANATION OF PLATE III

A schematic diagram of the measuring column showing the various foil positions in relation to the source location

PLATE III

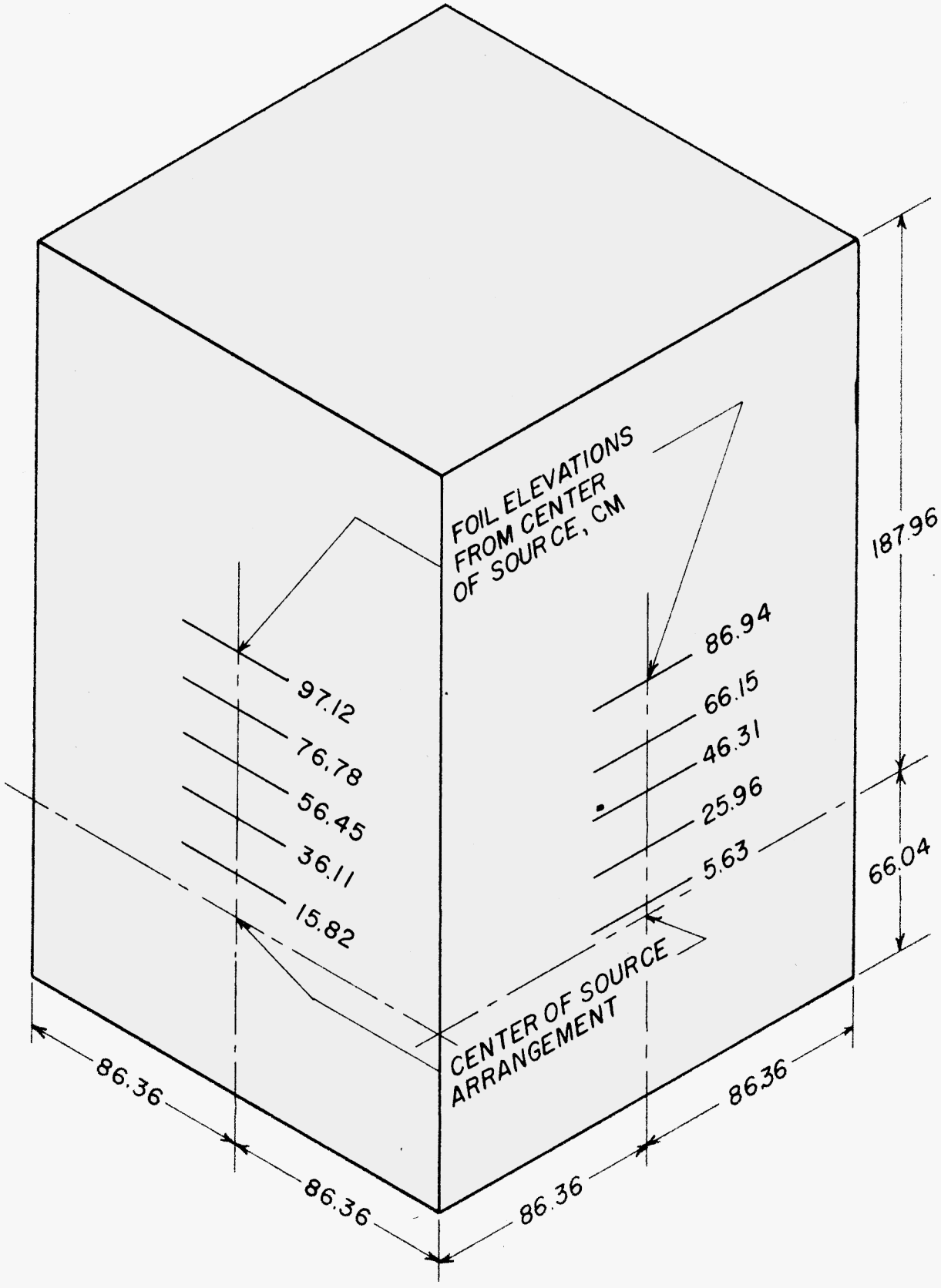
FOIL ELEVATIONS FROM CENTER OF SOURCE, CM
97.12
76.78
56.45
36.11
15.82
86.94
66.15
46.31
25.96
5.63
187.96
66.04
CENTER OF SOURCE ARRANGEMENT
86.36
86.36
86.36
86.36

sources fit snugly in the cylinders and of outer diameter such that the cylinders fit closely in the column's fuel ports. The sources, in their graphite positioning cylinders, were located in the column in the bottom row of fuel ports (just above the pedestal) such that the central axis along the length of the source containers coincided with the horizontal central axis of the fuel port, and also so that the center of the source coincided with the vertical central axis of the column. In this position, the center point of the source arrangement was approximately 26 inches from the bottom, 74 inches from the top, and 34 inches from any side of the column.

The indium foils were 1.00 inches in diameter, had a thickness of approximately 0.005 inches and weighed an average of 0.4592 grams, giving a mg/cm^2 thickness of 0.927. The foils were chosen such that their weights did not differ by more than one per cent.

The cadmium boxes, shown in Plate IV, were constructed by pressing them from cadmium sheet. The boxes had an inside diameter of slightly more than 1 inch and a wall thickness ranging from 0.021 inches to 0.022 inches. In addition to the cadmium boxes, the foils were covered on both sides with cadmium disks of the same thickness as the walls, giving an overall average cadmium cover thickness of 0.043 inches.

The foil stringers, 0.125 inches by 0.325 inches by 12 inches, shown in Plate II, were constructed from the same material as the graphite blocks. The stringers were recessed such that the

EXPLANATION OF PLATE IV

Photograph of cadmium covered foil arrangement

Legend:

A. Cadmium box base

B. Cadmium disk

C. Indium foil

D. Cadmium box cover

PLATE IV

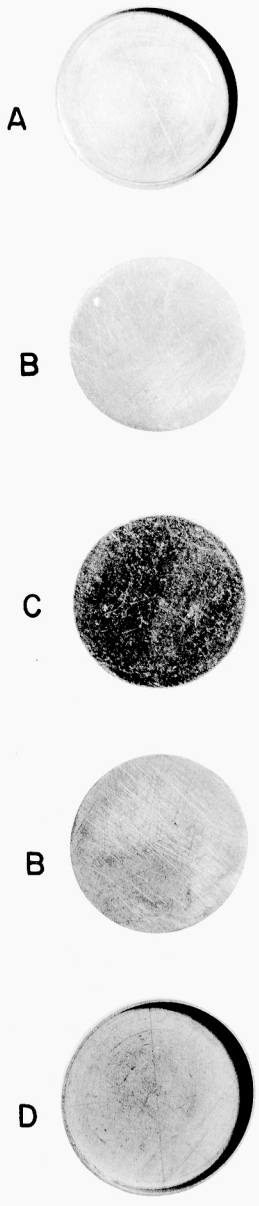

EXPLANATION OF PLATE V

Photograph of foil counting arrangement

Legend:

A. Gas flow counter in lead brick shield

B. Proportional counter preamplifier

C. Timer

D. Scaler

PLATE V

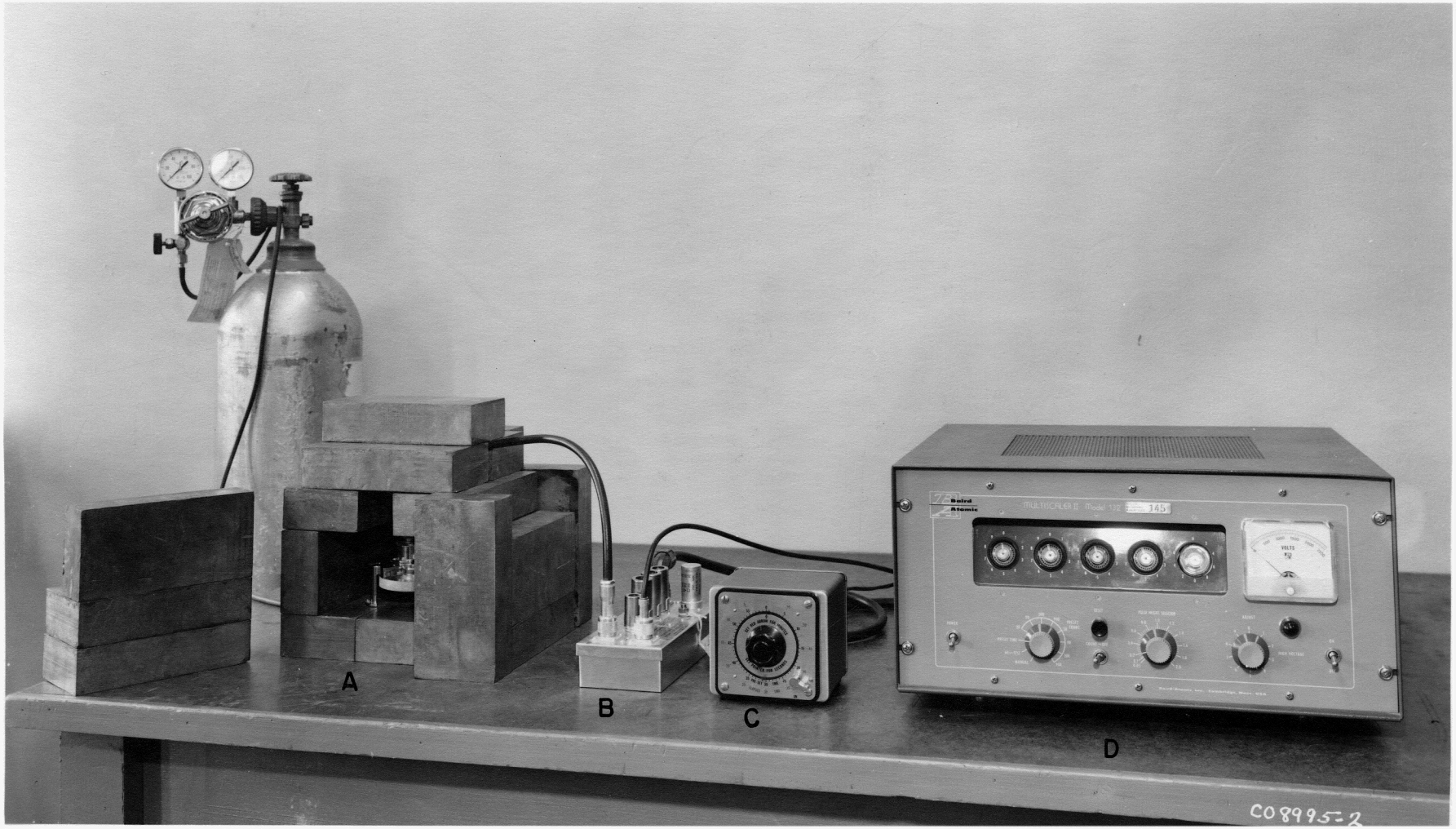

EXPLANATION OF PLATE VI

Close-up photograph of gas flow counter and lead brick shield

PLATE VI

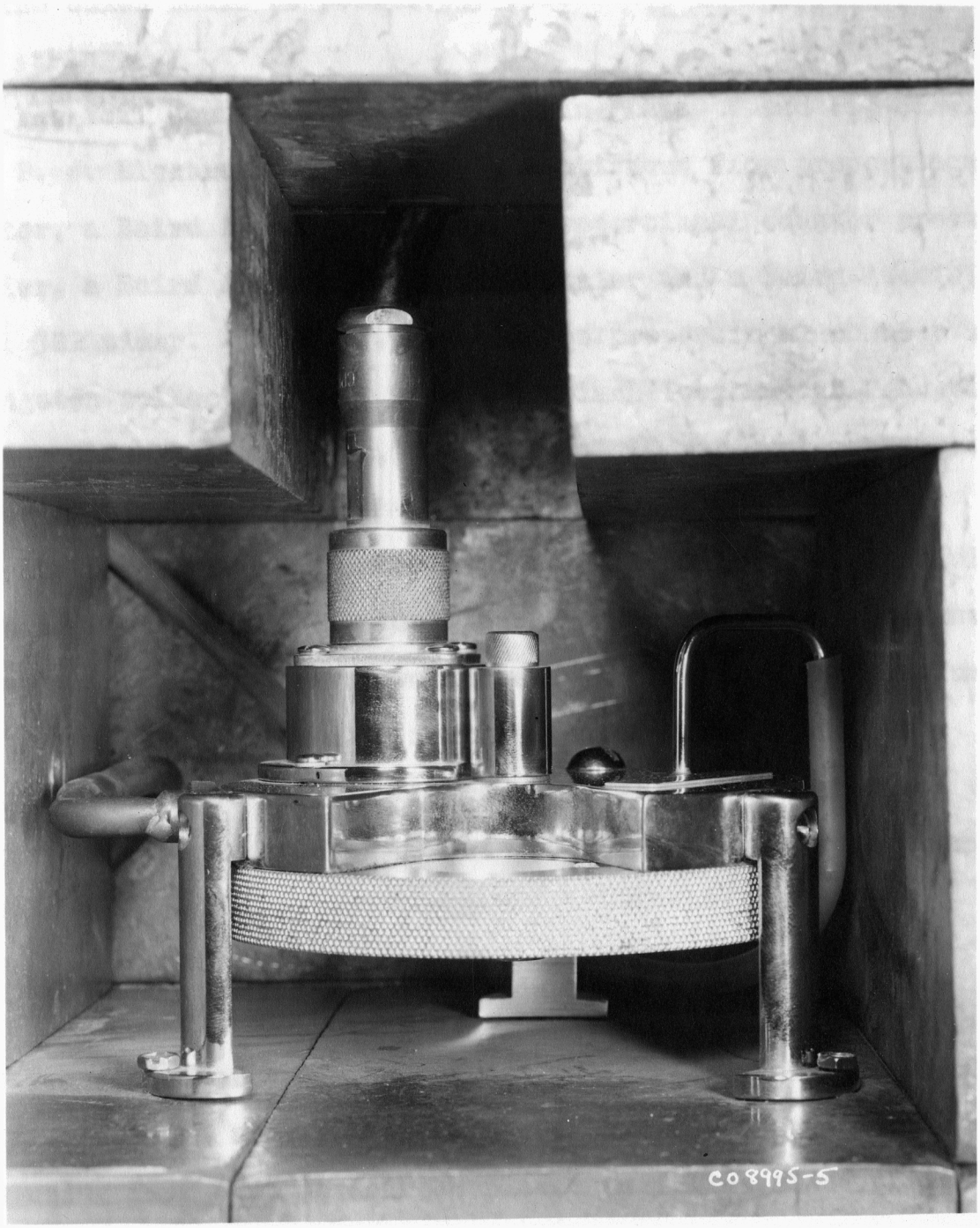

cadmium boxes could be positively positioned in the center of each stringer.

The foil counting system, shown in Plates V and VI, consisted of a B. J. Electronics, model DD7, continuous flow proportional counter, a Baird Atomic, model 255, proportional counter preamplifier, a Baird Atomic, model 322, scaler and a Baird Atomic, model 322 timer. The B. J. Electronics proportional counter had a tungsten collector wire, with a 1/2-inch loop and the counting gas was Olin-Matheson P-10, a mixture of 10 per cent methane and 90 per cent argon.

The proportional counter was housed in a lead brick shield, shown in Plates V and VI, such that the minimum shield thickness at any point was at least two inches. A 0.020 inch thick aluminum tray was constructed to facilitate the removal and the positioning of the foil in the counter well. The spacer was used to give the proper spacing between the foil and the collector wire.

Procedure

Two series of experiments were performed. The first series was made using a single neutron source and the second series was made using four neutron sources placed in a line along their axes. The series of experiments using one neutron source will be described first.

The single source was placed in position in the column as described under experimental apparatus. The foils, in their

cadmium boxes, plus the additional cadmium disks, were placed in the foil stringers and the foil stringers were then placed in the column such that the indium foils were centered on a line along the vertical central axis of the column, directly above the center of the neutron source. The foils were spaced such that the first foil was approximately 5 cm from the source with the remaining foils being spaced at approximately 10 cm intervals above the first, except for the seventh foil above the source, which was 9.70 cm from the sixth foil and 10.63 cm from the eighth foil. Ten foils were placed in the column at one time; the last foil being approximately 97 cm from the center of the source. A new set of foils was used at the start of the series of experiments and a given foil was always used in the same position. This was done to maintain the lowest possible counter background relative to the activity being measured.

The foils were allowed to remain in the column until they reached equilibrium saturation activity with respect to the 54 minute half-life isotope. The foil nearest to the source was removed and a spare foil, in an identical cadmium box, was placed in the vacated position. The foil, which was removed, was allowed to "cool" for 3 minutes to assure the decay of the 13 second half-life isotope and was then counted for a period of 27 minutes. At the end of the counting period, the foil, second closest to the source, was removed and the foil which had just been counted was put in the position vacated by the removed foil. The removed foil was then counted in the same manner as the first

foil. This procedure was followed until all ten of the foils had been counted. The foils were then all replaced to their original positions and allowed to again attain their equilibrium saturation activity. A total of eleven sets of data were taken using this same procedure. Of these eleven trials, 5 were made counting the activity of the source side of the foil and 6 were made counting the side of the foil away from the source. The background count was taken for a period of 27 minutes before and after the counting periods for each of the sets of data.

The counting system was checked for stability, before and after each trial, with a standard Ra-D-E source. The stability of the counting plateau was periodically verified. The counter was operated at 1950 volts and with a pulse height sensitivity of 0.2 volts. A number of trials were made using various sensitivity settings, foil-collector wire spacings and sizes of collector wire loops, to obtain an optimum operating plateau and minimum counter background.

A series of six trials was also made to determine the extent of the activation of the foils by other than the 1.44 ev resonance neutrons. The indium foils were covered on both sides by indium foils of the same thickness as the original foils, in addition to the usual cadmium boxes and disks. Four of the six trials were made by placing the foils in every other position, starting with the position closest to the source. Of the four trials, two were made counting the activity from the source side of the foils and two were made counting the activity from the

side of the foil away from the source. The remaining two trials were made by placing the foils in every other position, starting with the second position. One each of these trials was made counting the activity from the source side of the foil and the side of the foil away from the source.

After the series of experiments just described were completed, the foils were allowed to remain out of the pile for a day and were then counted to determine the amount of long life activity present.

At the completion of the trials for one source, four sources were placed in the column in the manner described previously under experimental apparatus.

A series of 13 trials was made using the 4 sources. Of these 13 trials, 7 were made counting the activity of the source side of the foil and 6 were made counting the activity from the side of the foil away from the source. The same procedure was used in the trials with four sources as was used in the trials for one source, except for the length of the counting periods. In the case of the four sources, each foil was counted for a period of twenty minutes and the background was counted for a period of twenty minutes before and after counting each set of data. At the end of the series of trials, the long life background was again determined as it was in the case for the single source trials.

Another series of three trials was made to determine the relative effect of the thickness of the cadmium covers on the

foil activities. The trials were made with four sources and the same procedure was used as described previously for four sources, except that the indium foils were placed in the cadmium boxes without the additional cadmium disks. These three trials were made counting the activity from the source side of the foil only.

Evaluation of Data

The data, obtained for the activities of the foils, was corrected for background and tabulated in Tables 1 and 2 for the single source and four source trials, respectively. The tabulated data in these tables is given as the total number of counts obtained at each position for all trials at that position, along with the average number of counts per trial at each position. The number of trials at each position, as given in the tabulated data, varied because some of the data had to be rejected on account of errors in experimental procedure such as timing, loss of gas pressure, counter voltage and background interference. If the data for one position in a set of data had to be discarded, the set of data, less the discarded data, was still used in the overall summation of counts at the individual positions. This procedure was deemed to be valid as the standard source activities showed that the counting system was stable between trials. Therefore, except for statistics, the total relative count rate distribution should not have been altered by leaving out the data from various points in individual sets of data.

In Fig.'s (1) and (2), for the single and four source

Table 1. Summary of experimental data obtained with a single source and corrected for background.

Distance r, cm	Summation of counts for all trials: a, side of foil*: No. of trials	a, side of foil*: Total counts	b, side of foil*: No. of trials	b, side of foil*: Total counts	Average counts for all trials: side a	Average counts for all trials: side b	Average of total counts for both sides of foil
5.63	5	174,531	6	210,964	34,906	35,161	35,034
15.82	5	139,292	6	163,288	27,858	27,215	27,536
25.96	5	95,365	6	107,034	19,073	17,839	18,456
36.11	5	55,289	6	62,120	11,058	10,353	10,706
46.31	5	29,581	5	27,098	5,196	5,420	5,668
56.45	5	13,053	5	11,820	2,611	2,360	2,488
66.15	5	6,603	6	7,046	1,311	1,174	1,248
76.78	5	2,493	6	2,752	499	459	479
86.94	5	1,141	6	1,284	228	214	221
97.12	4	513	6	526	128	87.7	107.8

*a - Side of foil facing source

*b - Side of foil facing away from source

Table 2. Summary of experimental data obtained with four sources and corrected for background.

Distance r, cm	Summation of counts for all trials: a, side of foil*: No. of trials	a, side of foil*: Total counts	b, side of foil*: No. of trials	b, side of foil*: Total counts	Average counts for all trials: side a	Average counts for all trials: side b	Average of total counts for both sides of foil
5.63	5	530,071	5	537,889	106,014	107,578	106,796
15.82	7	632,978	4	352,136	90,425	88,034	89,230
25.96	7	430,114	5	291,663	61,445	58,333	59,889
36.11	7	251,398	6	198,775	35,914	33,129	34,522
46.31	7	128,576	6	100,251	18,368	16,708	17,538
56.45	7	58,191	6	44,813	8,313	7,469	7,891
66.15	6	23,006	6	20,582	3,834	3,430	3,632
76.78	7	10,830	6	6,780	1,547	1,356	1,452
86.94	6	4,117	5	3,073	686	615	652
97.12	7	2,100	5	1,398	300	280	290

*a - Side of foil facing source

*b - Side of foil facing away from source

geometries, respectively, the average counts at each position were plotted versus the distance from the source and the source correction factors were determined as explained in the Appendix. The correction factors were plotted in Fig. (3), as a function of distance from the source, for both source geometries.

The activities, obtained for the trials made with indium foils covered with indium plus cadmium, were so low that it was not possible to obtain a meaningful correction for the activity induced in the foils by other than 1.44 ev resonance neutrons.

The measured activities, A, corrected for background and geometry were listed in Table 3, for both the single and four source geometries. The corrected activities, for the four source geometry, were normalized to the single source geometry, at 46.31 cm. These normalized activities, along with the corrected single source activities, were plotted versus r, in Fig. (4) and a smooth curve was drawn through the points so as to give the best curve through the single source geometry points from 0 to 46.31 cm and through the normalized four source geometry points from 46.31 cm to 96.12 cm.

Comparison of the normalized four source points with the single source points, showed that the two sets of points agreed reasonably well at intermediate distances, just beyond the point of normalization. However, for distances less than the point of normalization, the four source geometry points fell somewhat above those of the single source geometry, except at the first data point, where the two were almost equal and for distances

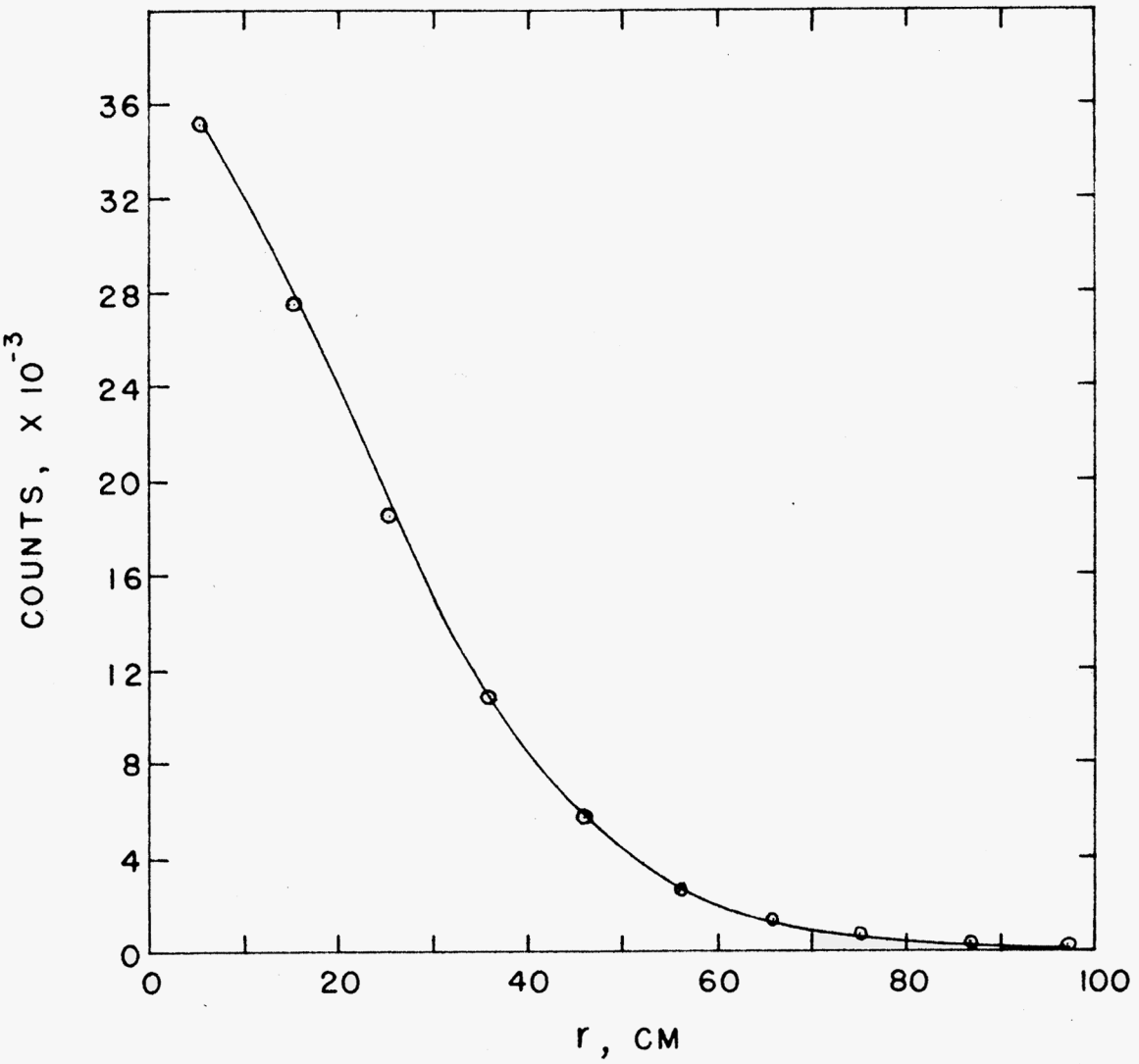

Fig. 1. Measured resonance neutron distribution for single source, corrected for background.

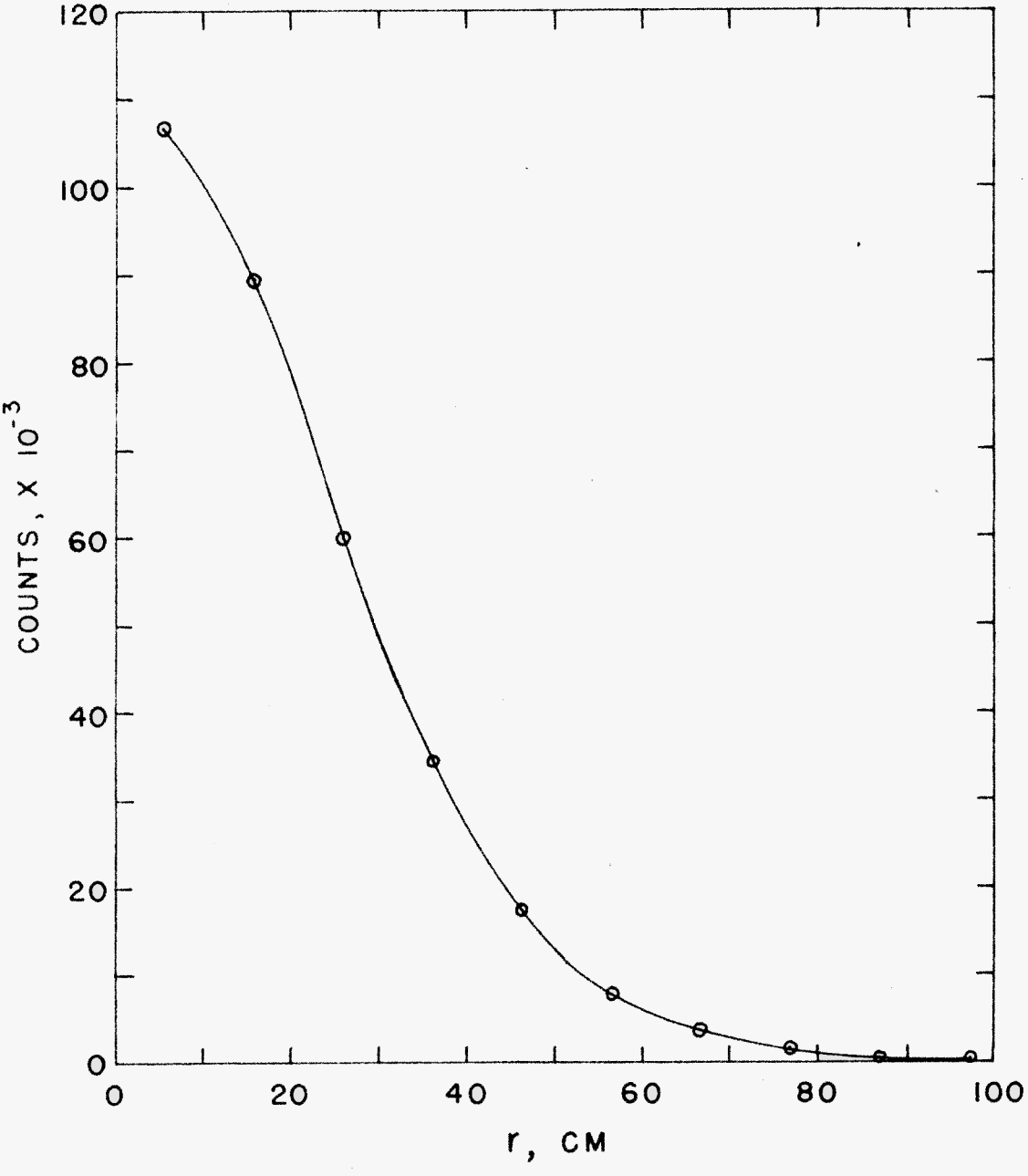

Fig. 2. Measured resonance neutron distribution for four sources, corrected for background.

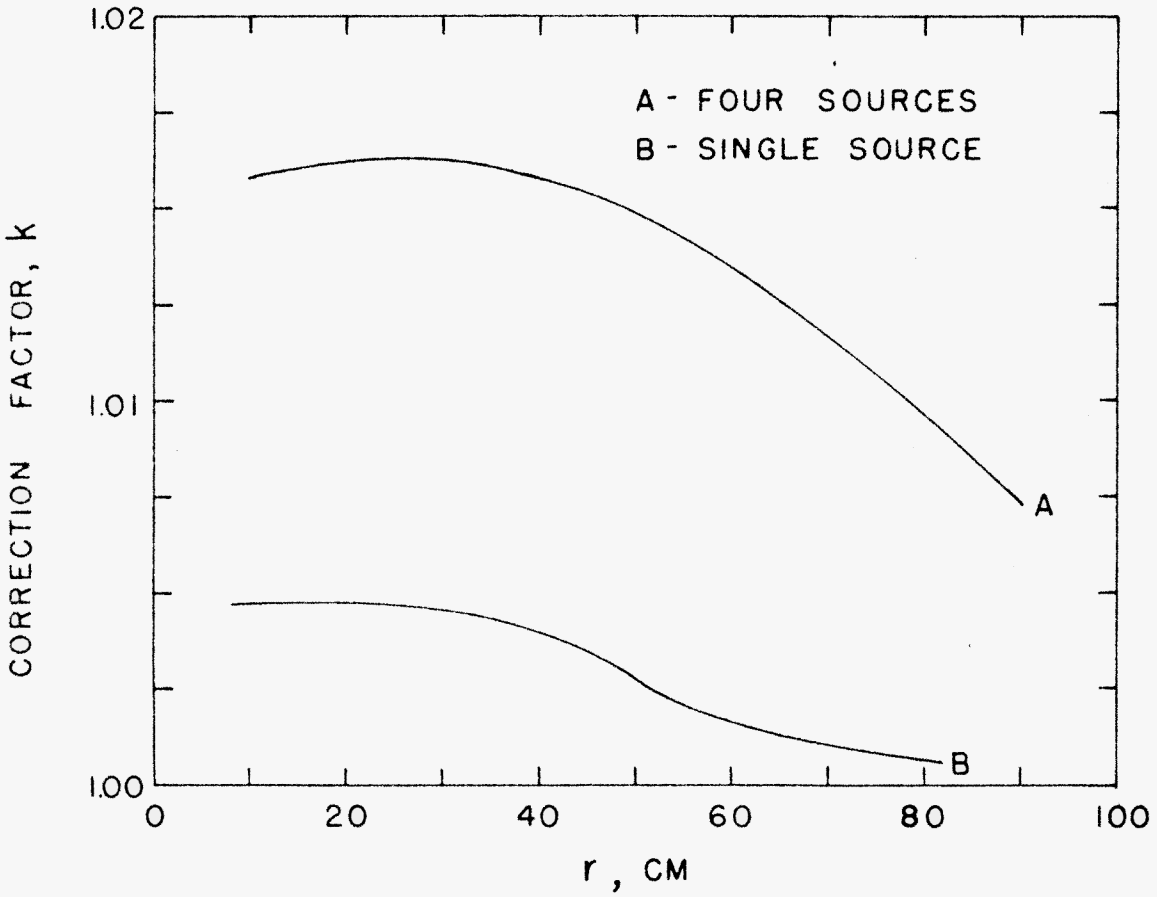

Fig. 3. Source and detector geometry correction factors for the single and four source distributions.

Table 3. Measured activities, A and Ar^2, corrected for background and geometry, for the single and four source geometries.

Distance r, cm	Single source A	Single source Ar^2	Four sources A	Four sources Ar^2
5.63	35,205	1.116×10^6	108,454	3.438×10^6
15.82	27,647	6.92	90,691	22.70
25.96	18,534	12.49	60,855	41.01
36.11	10,752	14.02	35,077	45.74
46.31	5,690	12.20	17,757	37.62
56.45	2,490	7.94	8,001	25.50
66.15	1,248	5.47	3,677	16.09
76.78	479	2.82	1,467	8.65
86.94	221	1.67	655	4.95
97.12	108	1.019	291	2.74

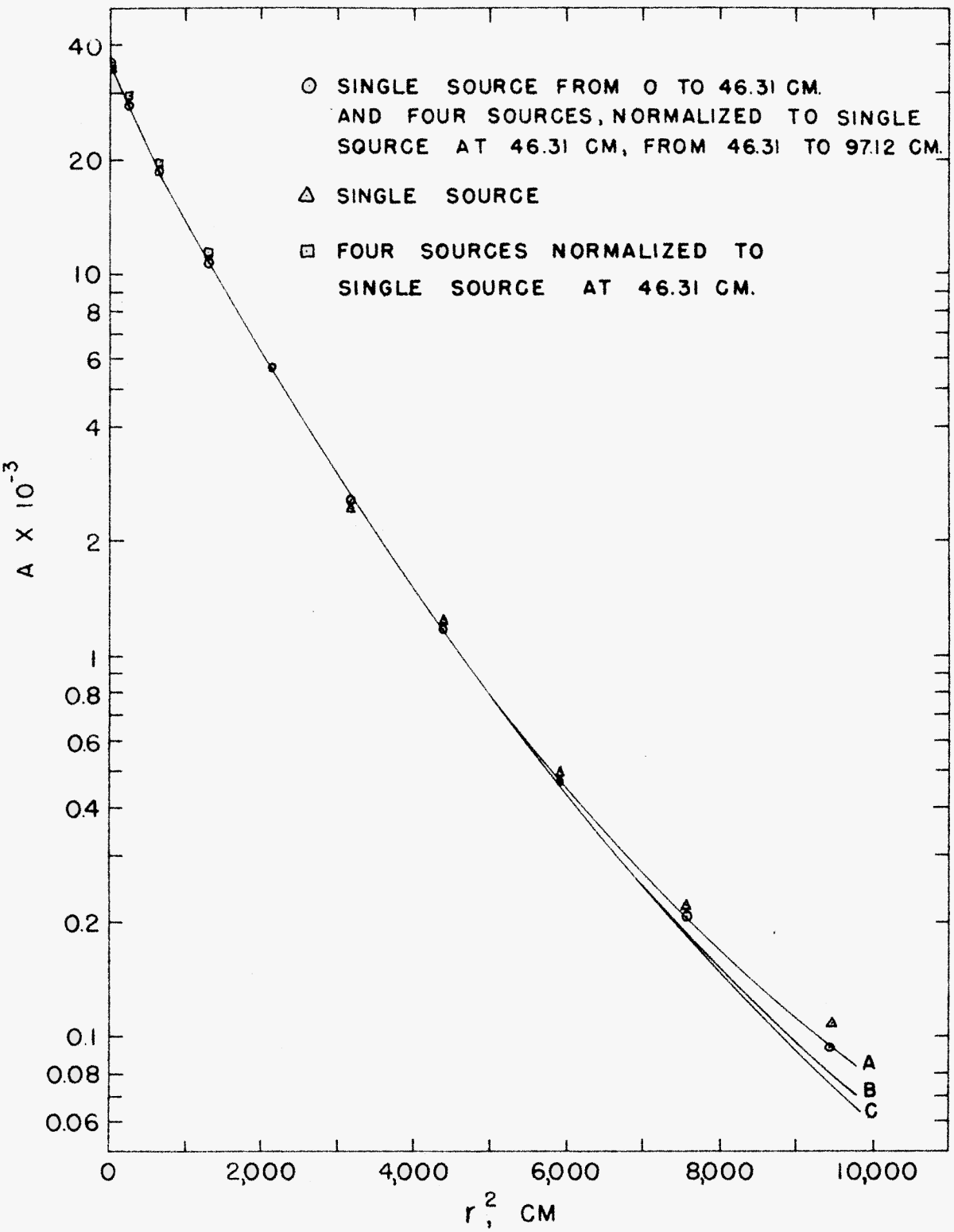

Fig. 4. Ln of the corrected indium resonance neutron distribution, A, versus r^2. Curves B and C show the results of subtracting 15 and 20 counts, respectively, from the original corrected distribution given by curve A.

far out, the single source geometry points fell above the four source geometry points. Close to the source, the points for the single source were probably the better representation of the true distribution, as the single source more nearly represented a point source and the source correction approximation was, therefore, more exact. Far out from the source, however, the source geometry should no longer have had a large influence on the distribution and, therefore, because of the greater activity of the foils for the four source geometry, and the resulting better statistics, the distribution as given by the four sources was taken to be the most meaningful far from the source.

The plot of ln Ar^2 versus r, as given by curve A in Fig. (5), was constructed by taking values of ln A versus r^2 from the plot of ln A versus r^2, given by curve A in Fig. (4). This method for plotting the ln Ar^2 versus r curve, was used because the shape of the ln A versus r^2 curve gave a better indication of where a curve should be drawn through the experimental points. Investigation, of the resulting ln Ar^2 versus r curve, showed that it started to curve upward at about 65 cm from the source and that the slope, given by the points near the outer end of the curve, was much less than that predicted by the expected exponential decrease in the distribution far from the source. Because of the very low counting rates, far from the source, it was assumed that there could have been a small constant systematic error in the background, due to residual foil activity or foil impurities, which would account for the slope of the curve

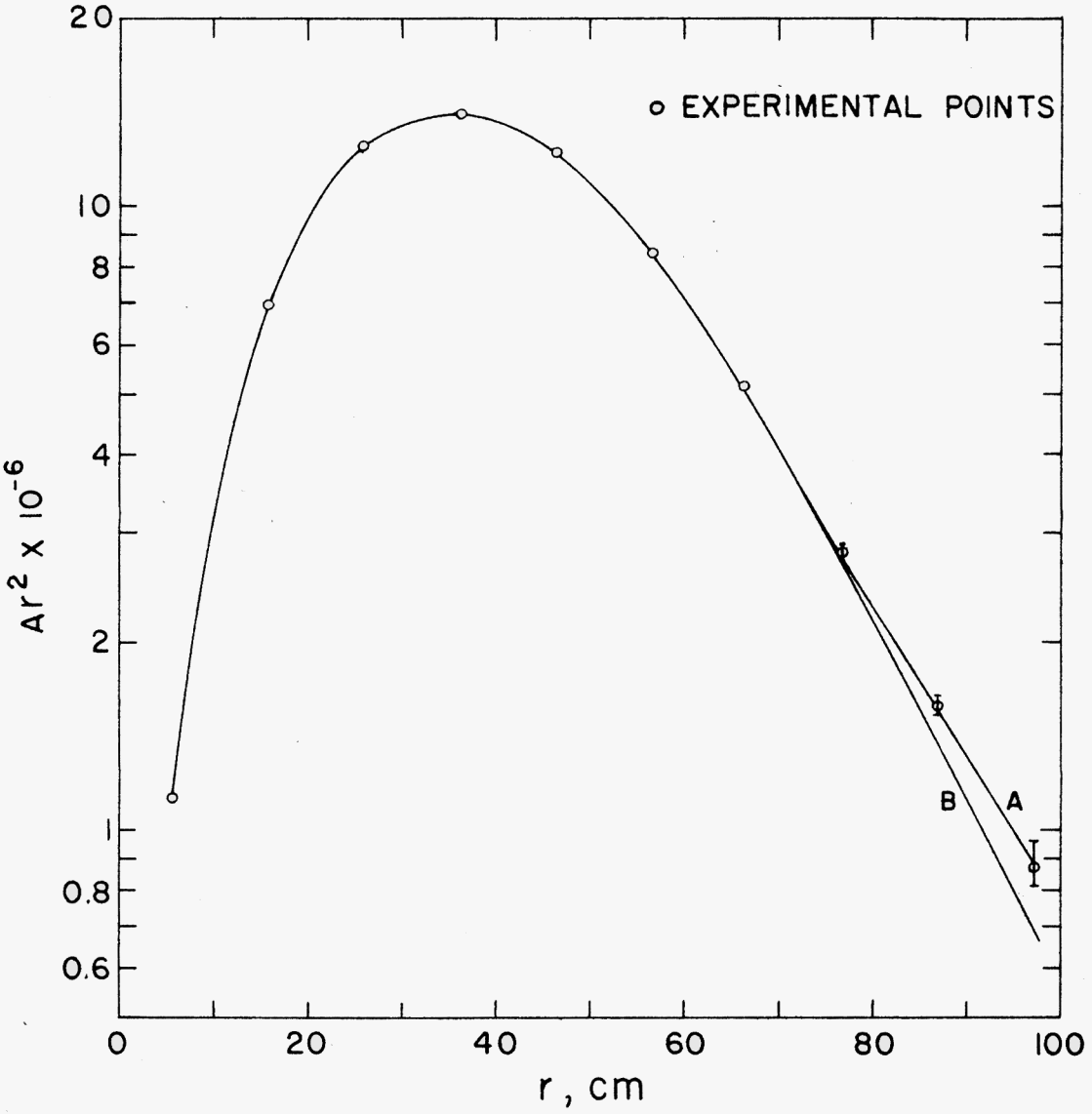

Fig. 5. Ln Ar^2 versus r for the corrected neutron resonance distribution.

Curve A. Distribution as given by curve A in Fig. (4).

Curve B. Distribution as given by curve C in Fig. (4).

obtained. Proceeding on the basis of the assumption of a constant background error, constant values of activity were subtracted from the values of the activity as given by curve A of the plot of ln A versus r^2. The curve of ln A versus r^2 was then replotted to correspond to the new values of the activities. Values of the new activities were then read from the new curve of ln A versus r^2, multiplied by r^2 and the curve of ln Ar^2 versus r replotted. This procedure was continued until the curve of ln Ar^2 versus r began to curve downward, instead of upward, at about 70 cm. This change occurred with a subtraction of 20 counts from the original activities. Curves B and C, of Fig. (4), show the results of the subtraction of constant activities of 15 and 20 counts, respectively, on the ln A versus r^2 curve and curve B, of Fig. (5), shows the final result of the subtraction on the ln Ar^2 versus r distribution. Curve B, of Fig. (5), was taken to be the true distribution and it was this curve that was used to calculate the final age. The values of Ar^2, from 0 to 5.63 cm, were obtained by plotting the assumed true Ar^2 versus r distribution on linear coordinate paper, and extrapolating from 0 to 5.63 cm, as shown in Fig. (6). To aid in the integrations indicated by Eq. (6), values of Ar^2 were read from the ln Ar^2 versus r curve and the extrapolated portion of the Ar^2 versus r curve, at 2 cm intervals, and were listed in Table 4. The integrations from 0 to 96 cm, were performed by numerical methods, using Simpson's rule.

To perform the integrations from 96 cm to ∞, the ln Ar^2

versus r curve, beyond 96 cm, was taken to be a straight line drawn through the last portion of the ln Ar^2 versus r curve. The expression for the straight line portion of the curve was

$$Ar^2 = k e^{-r/\lambda}$$

where λ and k were determined from the slope of the straight line extrapolation and the value of Ar^2 at r = 96 cm. The values of λ and k were determined to be

$$\lambda = 14.46 \text{ cm}$$

$$k = 7.246 \times 10^8$$

The integrals of Ar^2 and Ar^4, from 96 cm to ∞, were given as

$$k\int_{96}^{\infty} e^{-r/\lambda}\, dr$$

and

$$k\int_{96}^{\infty} r^2 e^{-r/\lambda}\, dr$$

respectively. The general form of these integrals is (7)

$$k\int_{r_0}^{\infty} e^{-r/\lambda} r^m dr = k\lambda e^{-r_0/\lambda} \sum_{i=0}^{m} \left[i!\, {}_mC_i\, r_0^{(m-i)} \lambda \right]$$

where n = 0, 2, 4, $\cdots$

and $${}_mC_i = \frac{m!}{i!(m-i)!}$$

Table 4. Values of Ar^2 versus r, read from curve B of the plot of ln Ar^2 versus r, given in Fig. (5), and the extrapolated portion of the linear plot of Ar^2 versus r, given in Fig. (6).

Distance r, cm	$Ar^2 \times 10^{-6}$	Distance r, cm	$Ar^2 \times 10^{-6}$
2	0.09	50	10.70
4	0.30	52	10.00
6	1.28	54	9.21
8	2.12	56	8.48
10	3.20	58	7.78
12	4.42	60	7.10
14	5.74	62	6.38
16	7.06	64	5.70
18	8.40	66	5.10
20	9.60	68	4.53
22	10.70	70	4.01
24	11.75	72	3.58
26	12.50	74	3.17
28	13.00	76	2.80
30	13.50	78	2.48
32	13.75	80	2.09
34	13.90	82	1.92
36	14.00	84	1.68
38	13.80	86	1.48
40	13.55	90	1.13
42	13.20	92	0.99
44	12.80	94	0.86
46	12.25	96	0.948
48	11.50		

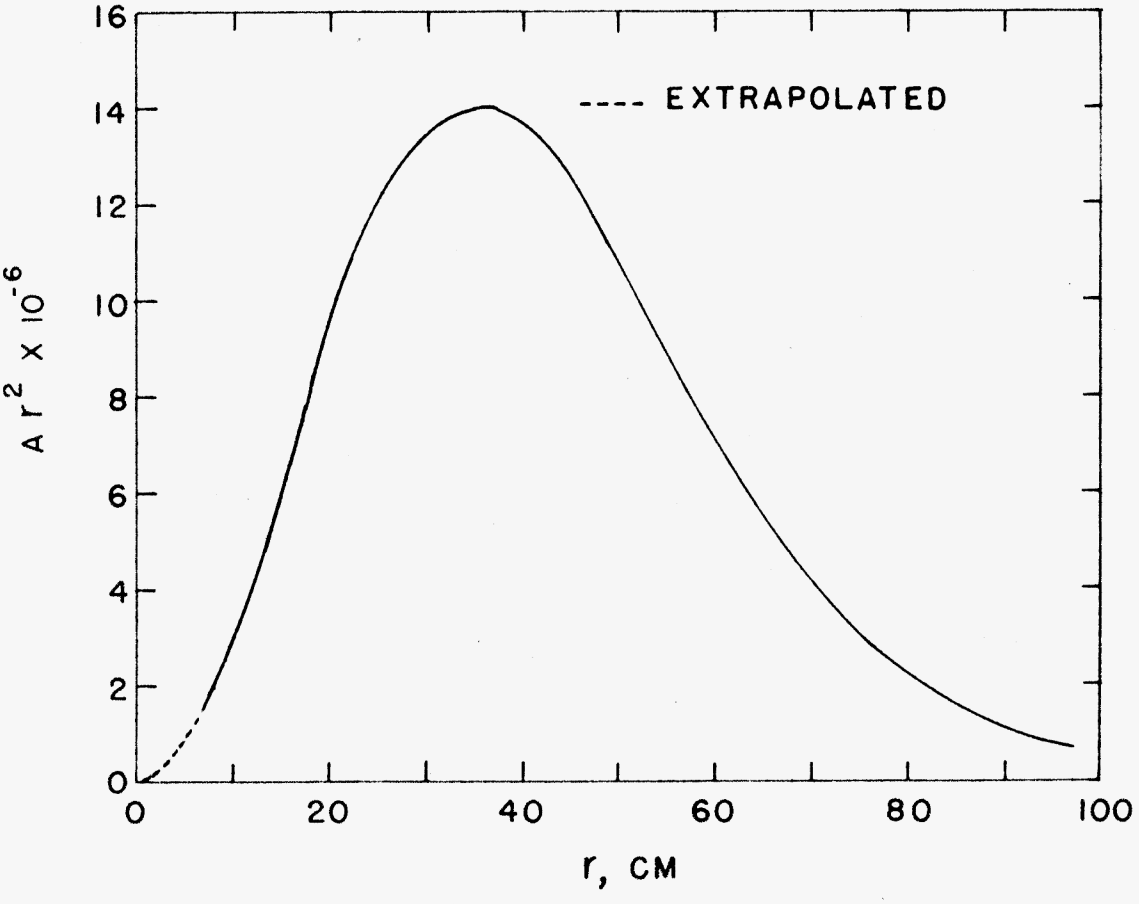

Fig. 6. Corrected Ar^2 versus r resonance distribution as given by curve B of Fig. (5).

By writing the expression for τ in the form

$$\tau(E_o,E) = \frac{1}{6} \frac{\int_0^{96} A r^4 dr + k\int_{96}^{\infty} r^2 e^{-r/\lambda} dr}{\int_0^{96} A r^2 dr + k\int_{96}^{\infty} e^{-r/\lambda} dr}$$

and solving, the value of $\tau(E_o,E)$ was found to be 378.3 cm^2.

The values obtained for the areas under the Ar^2 versus r and the Ar^4 versus r curves, from 0 to 96 cm and from 96 cm to ∞, were listed in Table 5. The percentage of the total area of the curves, which was extrapolated, was also determined and tabulated in Table 5.

The data, obtained for the activities of the foils covered only with the cadmium boxes (no additional cadmium disks), used in the experiments to determine the effect of cadmium thickness, was corrected for background and the average counts at each position, for all the trials, were tabulated in Table 6. To make the comparison between the distribution given by the two different cadmium cover thicknesses, the ratio of the average activity obtained using the cadmium covers plus cadmium disks, to the average activity obtained using only the cadmium covers was determined at each position. These ratios were also tabulated in Table 6.

The density of the graphite blocks, used to construct the column, was 1.683 gm/cm^3. The percentage of air voids in the measurement region of the column was calculated to be approximately 0.3 per cent. The resulting average density, taking

Table 5. Area under the Ar^2 versus r and Ar^4 versus r curves, from 0 to 96 cm and from 96 cm to ∞ and the percentages of the total areas extrapolated beyond 96 cm.

Curve	0 to 96 cm : Area, cm^2	96 cm to ∞ : Area, cm^2	Percentage of total area extrapolated
Ar^2 versus r	650.8×10^6	13.71×10^6	2.11
Ar^4 versus r	133.8×10^{10}	17.01×10^{10}	12.71
		Total	14.82

Table 6. Results of the experiments made to determine the effect of cadmium thickness on the resonance neutron distribution.

Distance: r, cm	A, Cd boxes only	A, Cd boxes plus Cd disks	A(Cd boxes plus Cd disks) / A(Cd boxes only)
5.63	110,061	106,014	1.038
15.82	94,535	90,425	1.045
25.96	64,002	61,445	1.042
36.11	37,228	35,914	1.037
46.31	19,182	18,368	1.044
56.45	8,696	8,313	1.046
66.15	4,036	3,834	1.053
76.78	1,602	1,547	1.036

into account the air voids, was 1.678 gm/cm^3.

The age τ, as defined by the Fermi age theory, is inversely proportional to the square of the density. Therefore, the age, corrected to a density of 1.60 gm/cm^3, becomes 416 cm^2.

ANALYTICAL PROCEDURE

The age, in graphite, was calculated for four different neutron source spectra. These calculations were as follows:

1. Fission age from fission energies to 1.44 ev, using the fission spectrum determined by Cranberg, et. al., (3).
2. Pu-Be age from source energies to 1.44 ev, using the calculated spectrum of Hess (10).
3. Pu-Be age from source energies to 1.44 ev, using the experimental spectrum as determined by Stewart (16).
4. Po-Be age from source energies to 1.44 ev, using the experimental spectrum as determined by Whitmore and Baker (20).

The ages for the Pu-Be and Po-Be sources were calculated using Eq.'s (12) and (14). These calculations were carried out on the Kansas State University IBM 650 computer. A complete description of the computer program is given in the Appendix.

The source spectra, as given in the references for Pu-Be and Po-Be, were plotted as the relative number of neutrons, N(E), versus energy E, in Fig.'s (7) and (8), respectively. Values of N(E) were read from the plots at 0.1 Mev energy intervals, starting with 0.05 Mev. These values of N(E) were taken to be the average values in each 0.1 Mev interval and the area in each interval was calculated using the trapezoidal rule. The

individual areas were summed so as to give the cumulative area from 0 energy to each of the energies at which the values of N(E) were taken. These cumulative areas were divided by the total area of all the intervals, giving the cumulative fraction of neutrons, from 0 energy, to each of the energies for which cumulative areas were calculated. The cumulative fractions were plotted, versus energy, in Fig. (9). The fraction of neutrons between two source energies was taken to be the difference in the cumulative fractions at the two energies. The cumulative fractions, for the fission spectrum, were obtained from tabulated data in ANL-5800 (15), for the spectrum determined by Cranberg, et. al. (3). The cumulative fractions of fission neutrons, versus energy, were also plotted in Fig. (9). The average energies corresponding to the fractions, f_i, were read from the cumulative plots, for various fractions from 0 energy to the maximum source energies and were tabulated in Table 9, for the Pu-Be and Po-Be spectra and in Table 10, for the fission spectrum. The largest fraction taken for any interval did not exceed 0.01.

Data for the neutron cross sections in graphite were obtained from Supplement No. 1 to BNL-325, second edition; UCRL-5226; and NDA 12-16. The total cross sections, as given in these references, were plotted on a large plot shown in Fig. 12. Values of the cross sections were read from this plot such that the cross section, between any two values taken, was essentially a straight line. The values of the cross sections were tabulated

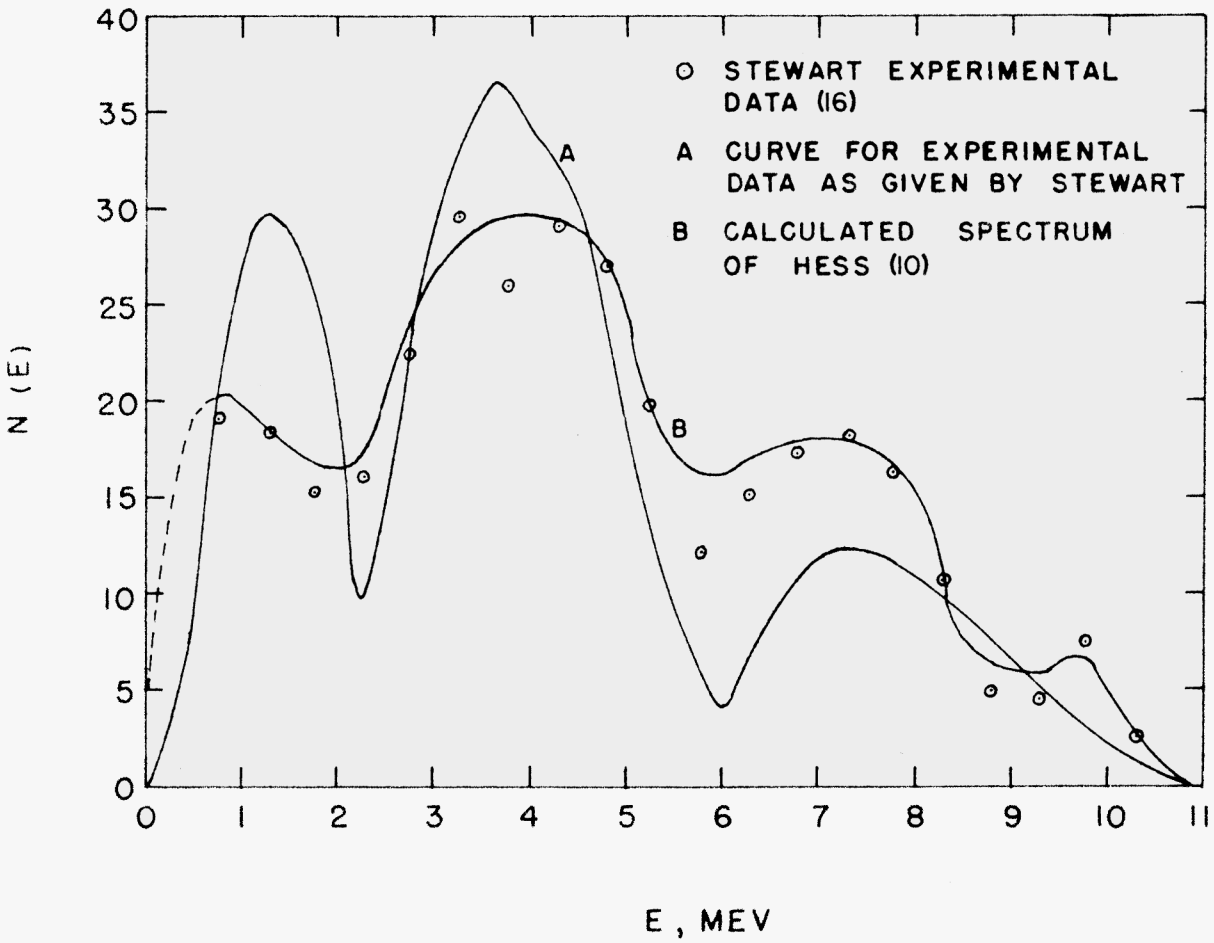

Fig. 7. Calculated and measured neutron energy spectra for a Pu-Be source, plotted as the relative number of neutrons versus energy.

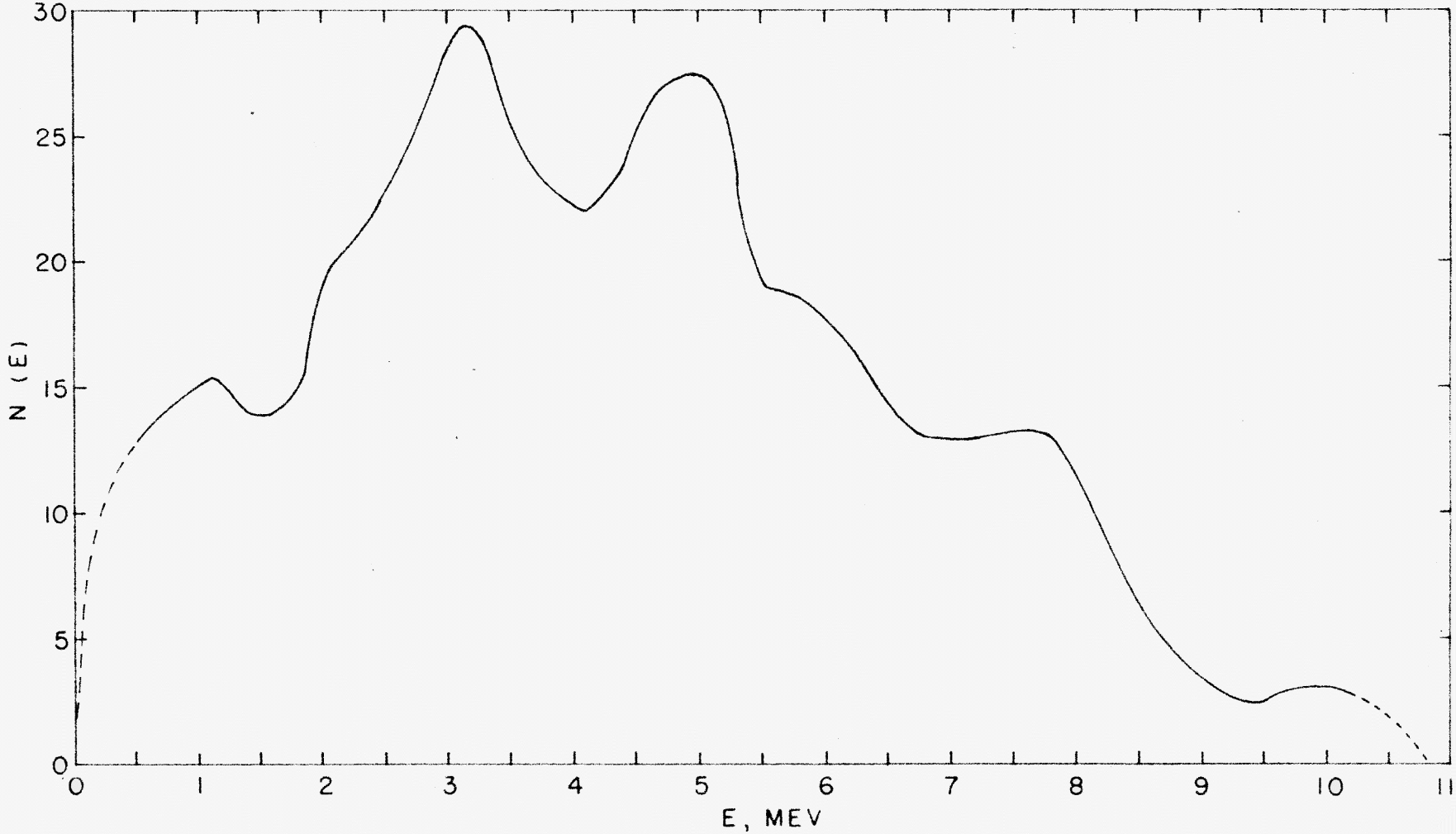

Fig. 8. Measured neutron energy spectrum for a Po-Be source as determined by Whitmore and Baker (20) and plotted as the relative number of neutrons versus energy.

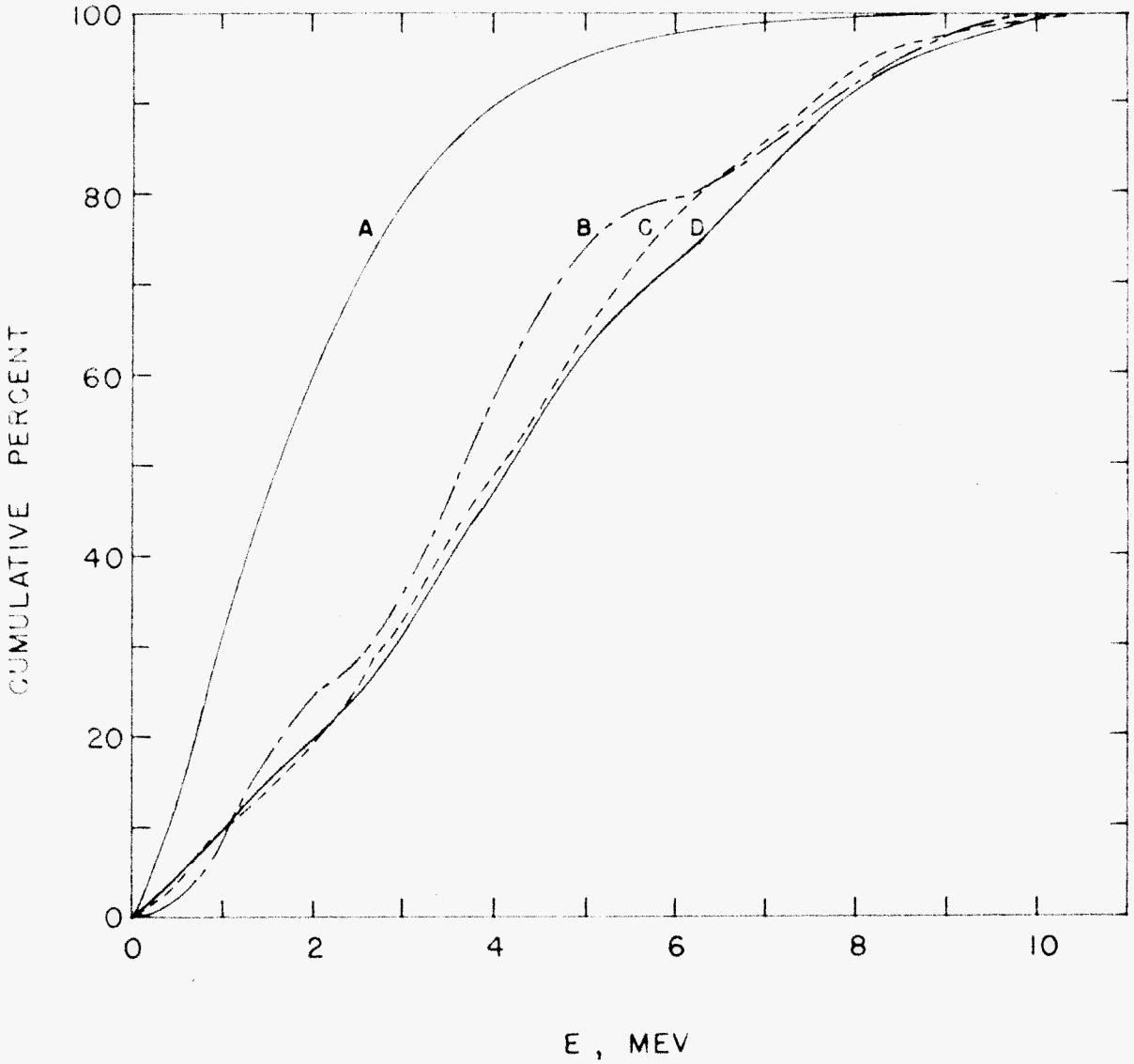

Fig. 9. Measured and calculated spectra for Pu-Be, Po-Be and fission neutron sources.

Curve A. Measured fission spectrum (3)

Curve B. Calculated Pu-Be spectrum (10)

Curve C. Measured Po-Be spectrum (20)

Curve D. Measured Pu-Be spectrum (16)

in Table 11, along with the corresponding energies.

The calculation of the ages for the various sources was carried out according to the procedure given in the theory and in the description of the computer program. The ages were calculated between the source energies and fission energies and were then added to the assumed correct value, 311 cm^2, for the experimental fission age to indium resonance, to obtain the total ages from source energies to 1.44 ev. The age from fission energies to 1.44 ev was also calculated in order to determine the accuracy of the method of calculation and to permit an estimation of the errors in the calculations. The monoenergetic fission ages, to 1.44 ev, as calculated from the fission spectrum energies corresponding to each fraction, f_i, of neutrons, were tabulated versus energy, both with and without the first collision correction, in Table 9.

The estimated errors in the calculated ages, for the Pu-Be and Po-Be source spectra, were obtained by assuming that the errors in the calculations from source energies to 1.44 ev, was twice the error obtained in the calculation of the fission age to 1.44 ev.

DISCUSSION OF DATA EVALUATION AND RESULTS

Because of the lack of data concerning the age of Pu-Be source neutrons in graphite, a comparison of the results obtained in this experiment was made to previously published results for the age of similar source neutrons in graphite.

The neutron spectrum from Pu-Be must be very close to the spectrum from Po-Be, because the alpha particles from Pu have energies of 5.15, 5.137 and 5.09 Mev, while Po has one alpha of 5.30 Mev. This slight difference in energy results in only a slight difference in the energy spectra of the two sources.

The calculated spectrum by Hess (10) and the measured spectrum by Stewart (16), for Pu-Be neutrons, is shown in Fig. (7). The measured spectrum for Po-Be neutrons, by Whitmore and Baker (20), is shown in Fig. (8).

The neutron spectrum, from Ra-α-Be sources, should also be very close to the spectrum for Pu-Be. The mean energy of Ra-α-Be neutrons was calculated to be 3.80 Mev (10), although reported to be larger than this for experimental determinations. The effective mean value for the Pu-Be neutrons, given by Stewart (16), for the experimental spectrum, was 4.4 Mev.

From the preceding considerations, the age for the Po-Be and the Ra-α-Be sources should not differ appreciably from that given by the Pu-Be sources. Valente and Sullivan (17) have reported the experimental age of Pu-Be neutrons in water to be 52.8 cm^2, compared to an age of 57.3 cm^2 for Po-Be neutrons. The two determinations being carried out with the same experimental apparatus. The average of six published measurements, as given by Bogart, Cusick and Shook (2) and cited in ANL-5800(1958) (15), gives the age of Ra-α-Be neutrons in water as 48.5 cm^2.

The available data for neutron ages in graphite was not as abundant as that given for water but a few comparisons of the

ages for the various sources in graphite were possible.

Data from the standard graphite pile, at Brookhaven National Laboratory for a Ra-α-Be source, and from measurements made by groups at the Oak Ridge School of Reactor Technology for a Po-Be source in graphite, analyzed by Bogart, Cusick and Shook (2), gave values of the age as 370 ± 20 cm^2 for Po-Be and 360 ± 10 cm^2 for Ra-α-Be sources. Bogart, Cusick and Shook (2) also reported calculated values for the age in graphite, for Po-Be and Ra-α-Be neutrons, based on a Monte Carlo technique and experimentally determined values for the spectra of the two sources above 1 Mev. The calculations were made by assuming various spectral components for the sources from 0 to 1 Mev. For the Po-Be source spectra with 0 to 1 Mev components of 3, 30, and 40 per cent, age values of 472, 405 and 380 cm^2, respectively, were obtained. For the Ra-Be source with 0 to 1 Mev components of 0, 50 and 60 per cent, age values of 481, 396 and 386 cm^2 were obtained. The value of the calculated age obtained for fission neutrons, in these calculations, was 313 cm^2, which compared very well with the usually accepted value of 311 cm^2.

Hughes (12) has reported the results of an experimental fit for the slowing down distribution from a standard Ra-α-Be source, to indium resonance, in the Argonne National Laboratory standard graphite pile. The fit was made by assuming that the distribution could be represented by a sum of three Gaussian slowing down kernels, for a point source in an infinite medium. The expression obtained for the actual slowing down density, as

measured by standard indium foils, was

$$q = 0.0017A = 16.4e^{-r^2/(27.12)^2} + 8.47e^{-r^2/(41.40)^2} + 0.13e^{-r^2/(65.00)^2}$$

where A was the activity of the foils. The results of the solution of this expression, for various values of r, were plotted in Fig. (10), along with a plot of the corrected distribution as determined in this experiment for a Pu-Be source. The Ra-α-Be distribution was normalized to the Pu-Be distribution at 70 cm. An inspection of the two curves shows that they agree quite well. The Ra-α-Be curve appears to fall off somewhat faster at the extreme end of the curve but lies somewhat above the Pu-Be curve close to the source. The validity of the Ra-α-Be curve, at great distances, is somewhat in doubt because it falls off faster than an exponential, due to the Gaussian nature of the kernels used to make the fit. A difference in the density of the graphite used in this experiment, 1.683 gm/cm^2, and that of the standard pile (not given by the quoted reference) could make a difference in the shape of the two curves and also could account for the difference in the measured ages. Amaldi (1) reported the value of the age, obtained by the use of this fit, to be approximately 380 cm^2, for the Ra-α-Be source neutrons.

The values for the calculated ages determined in this experiment, including the first collision effect as listed in Table 7 were 298.4, 421, 403 and 416 cm^2 for the fission (also including the last collision effect), experimental Pu-Be, calculated Pu-Be

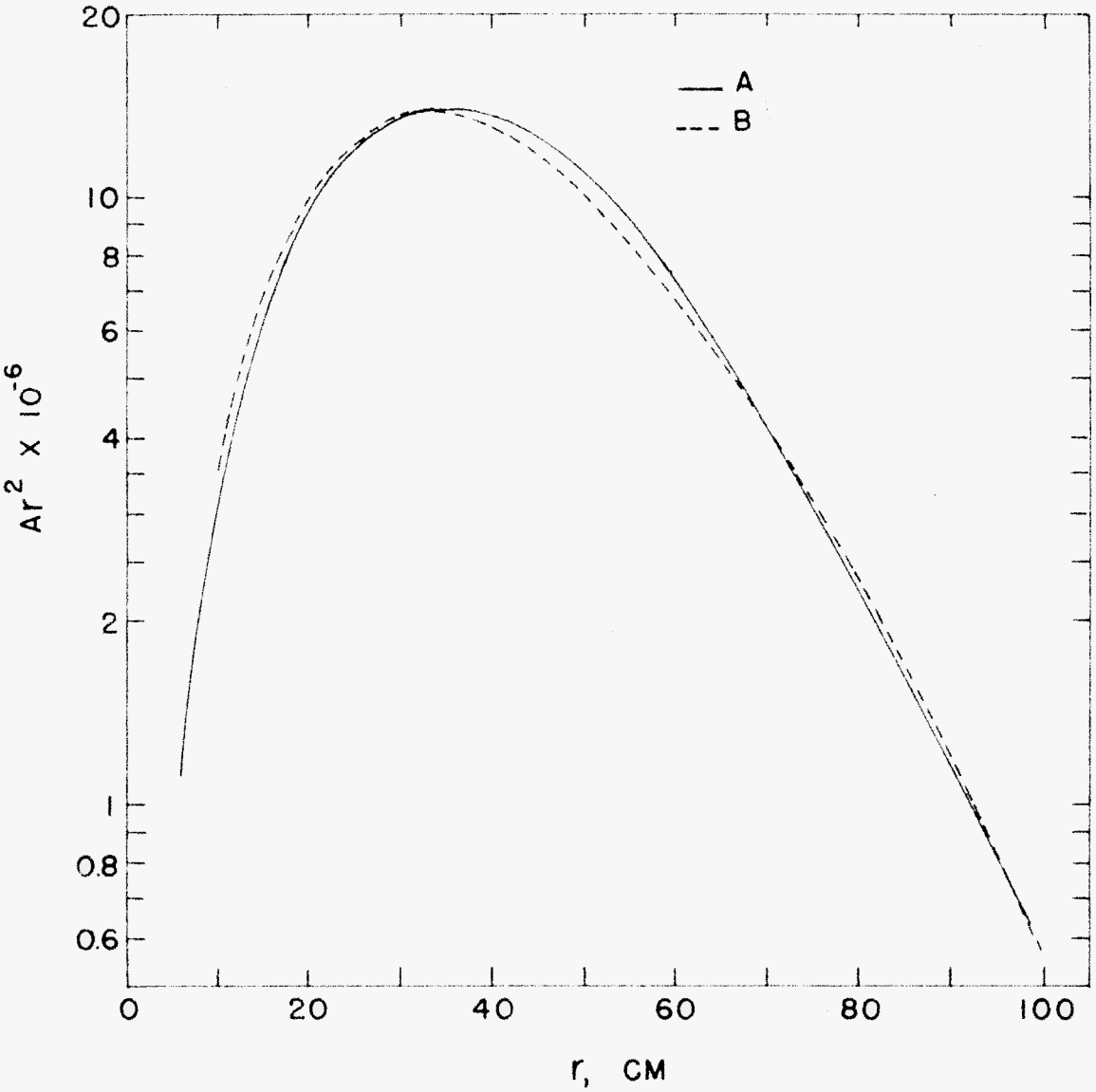

Fig. 10. Ln Ar^2 versus r for the measured resonance neutron distribution for Pu-Be and Ra-α-Be source neutrons.

Curve A. Distribution for Pu-Be source as given by curve C of Fig. (4).

Curve B. Resonance neutron distribution for a Ra-α-Be source as given by an empirical fit for the data obtained in the Argonne National Laboratory standard graphite pile (12).

Table 7. Summation of the results obtained in the age calculations, with and without the first collision correction, for the various source spectra, and the estimated error in the calculated ages, based on the assumption that the errors in the calculations from source to fission were twice the error in the calculation from fission to 1.44 ev, and that the correct fission age was 311 cm^2.

Source	Calculated age source to fission, cm^2		Total age to 1.44 ev, cm^2		Total estimated error, %	
	With correction	Without correction	With correction	Without correction	With correction	Without correction
Experimental Pu-Be (16)	111.2	100.6	422.2	411.6	2.31	4.42
Calculated Pu-Be (10)	92.3	85.1	403.3	396.1	1.85	4.21
Experimental Po-Be (20)	105.4	94.3	416.4	405.3	2.05	4.20
Fission (3), (to 1.44 ev)	298.4*	282.9			4.05	9.04

*Also includes the last collision correction

and experimental Po-Be sources, respectively. The last collision correction, for the fission age, was 2.35 cm^2, using a cross section of 4.7 barns at 1.44 ev.

The 0 to 1 Mev components, for the calculated and experimental Pu-Be spectra, were approximately 8.5 and 10 per cent, respectively. The 0 to 1 Mev component for the experimental Po-Be source, was approximately 9 per cent.

The comparison of the age obtained in this experiment, with the experimental ages previously obtained with similar sources, indicated that the value obtained in this determination was approximately 10 per cent too high. This comparison, however, cannot be conclusive as the exact details of the previous experiments were not known. The comparison of the experimental result with the previously calculated results for other sources and the results obtained in this study, showed that the experimental value agreed quite well with the calculated values, using the experimentally determined spectra, but was somewhat higher than the value obtained for the calculation using the calculated spectrum. Bogart, Cusick and Shook (2), by comparison of various experimental and calculated ages for various materials, argued that the experimentally determined neutron spectra for the Ra-α-Be and Po-Be sources, did not contain a large enough component of low energy neutrons. If this were also true for Pu-Be sources, then the value of the Pu-Be age, as determined in this experiment, would certainly be too large.

On the other hand, the age values calculated in the analyti-

cal portion of this study agreed quite well with the previously calculated ages, for similar sources, using the experimentally determined source spectra. The value obtained using the calculated Pu-Be spectrum was about 5 per cent less than that obtained using the experimentally determined spectrum. This also would indicate that the experimental spectral determinations do contain too large a component of high energy neutrons.

The limits of the errors in the experimental determination of τ are difficult to assess accurately because of the manner in which the different portions of the curves contribute to the second moment of the slowing down distribution, $\overline{r^2}$. The normalized experimental points, shown in Fig. (5), give the limits on the statistical counting errors encountered in determining the foil activities.

The various factors which have possibly contributed to the uncertainty in the final experimental value of τ are listed as follows:

1. Uncertainty in the source and detector geometry correction factors.
2. Effect of the cadmium cover thickness and the number and spacing of foils.
3. Possible long life foil activity.
4. Contribution to the foil activity by other than resonance neutrons.
5. Statistical uncertainty in the measured portion of the distribution.
6. Experimental uncertainty in graphite density and effect of voids in the measuring column.

The method of source correction, used in this experiment, has been successfully used in previous experiments and for similar geometries. It was somewhat difficult to evaluate the slope of the curve, close to the source, because the measured distribution had to be extrapolated from 0 to 5.63 cm. However, the error in this extrapolation should have been small and since the correction factors were also small, very little error should have been encountered in the correction for the single source. The distribution as given by the four sources, was not used for distances less than 46.13 cm and, therefore, should have been little affected by the source geometry.

The values, given in Table 6, for the ratios of the activities of the foils covered only with the cadmium boxes, to the activities of the foils covered with the cadmium boxes plus cadmium disks, showed that within statistical error, the relative spatial distribution was unaffected. These results also indicated that the foil spacing was adequate. Hill, Roberts and McCammon (9) have reported that a spacing of approximately 10 cm between foils should give only a relative effect on the spatial distribution.

The determination of long life foil activities indicated a noticeable amount of activity, but the statistics of the count rate did not allow for a meaningful correction. The measured activities were such that they appeared to be at least partially relative to the spatial distribution and, therefore, as long as a given foil was always used in the same location, no correction

had to be made. The count rate as a function of time after the removal of a foil from the column, for the series of experiments to determine the half life of the long life activity described in the experimental procedure, was plotted on semilog paper in Fig. (11). A least squares analysis of the experimental points produced a curve which gave a half life of 46 days for the measured activity. This half life was well within statistical error of the 49 day half life of indium 114.

The experiments with the self-shielded indium foils, made to determine the effect of the activity induced in the foils by other than resonance neutrons, were not successful. The counting rates for the foils, far from the source, were too low to obtain any meaningful correction factor.

The uncertainty in the extrapolated portion of the ln Ar^2 versus r curve was quite large. As previously explained, the shape of the curve far out, for the original distribution, began to curve upward at about 65 cm from the source. The shape of the curve indicated that perhaps there had been a constant systematic error in the experimental data due to background effects, such as residual and long life foil activities and contamination. Proceding on this assumption, constant values of activity were subtracted from the distribution, until the curve began to curve downward, instead of upward, at about 65 cm from the source. The amount of activity subtracted, 20 counts/counting interval, would have been approximately only 1 count/minute. In view of the measured background of approximately 10 counts/minute, the

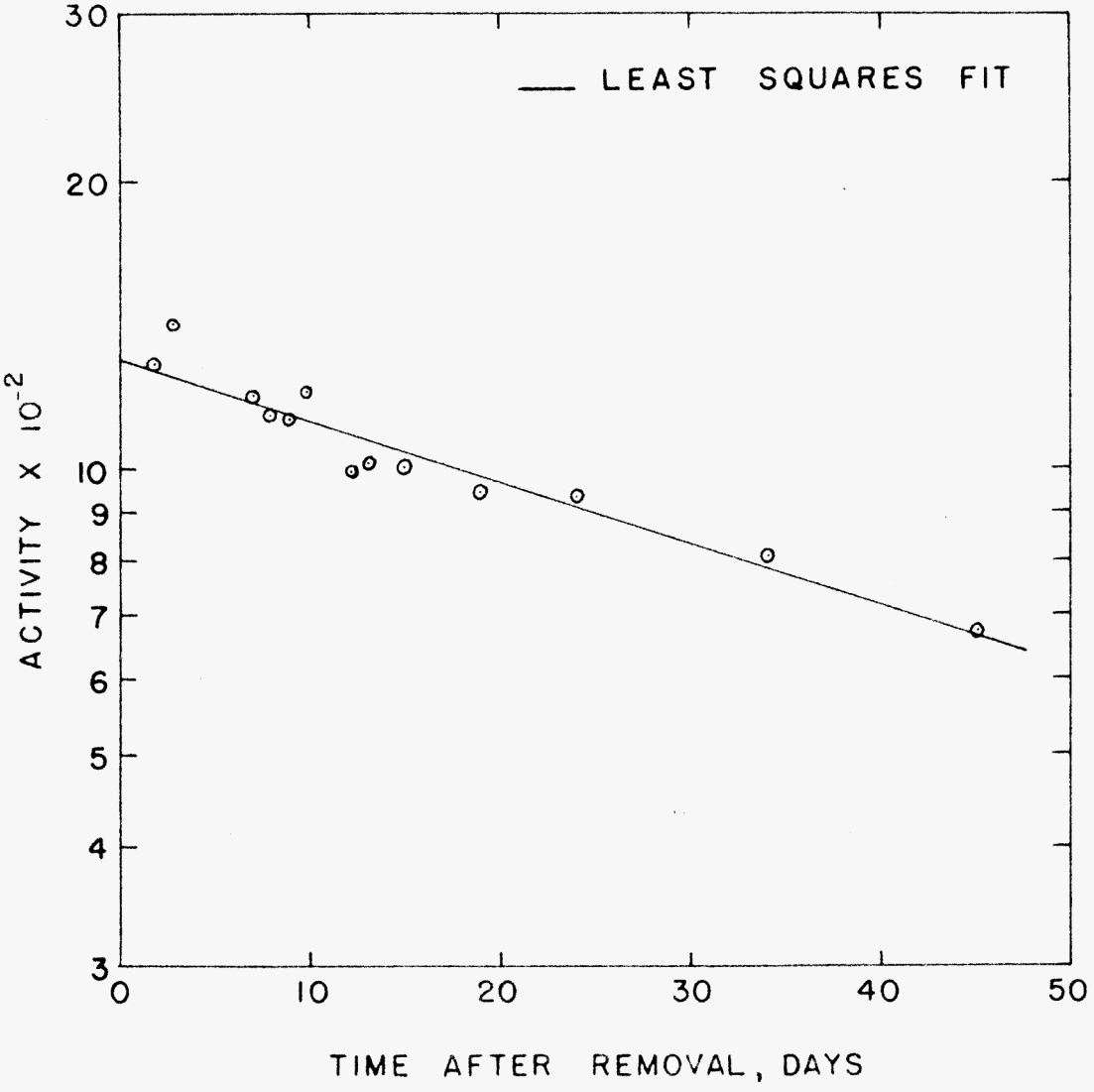

Fig. 11. Long life indium foil activity as a function of time after removal from the graphite column.

correction for the systematic error should not have been too extreme, although it pointed out the extreme sensitivity of the shape of the curve far from the source for the measured distribution.

The value of λ, obtained from the slope of the last portion of the corrected ln Ar^2 versus r curve, was 14.46 cm. This value of λ compares with the mean free path of approximately 10.8 cm, for high energy neutrons in graphite, and is, therefore, larger than the value predicted by the theory of the exponential character of the ln Ar^2 versus r distribution, far from the source. The high value of λ indicated that the slope of the last portion of the curve was too small. However, high energy neutrons in graphite can travel appreciable distances between the point of their first collision and the point at which they reach resonance energy. This would account for at least a part of the difference in the λ's.

The fraction of the total age obtained from the extrapolation of the ln Ar^2 versus r distribution beyond 96 cm was only 14.8 per cent, but this percentage changed rapidly with a change in λ or k and, therefore, it was still difficult to estimate an error in the age due to an error in the extrapolated portion of the distribution.

The uncertainty of the absolute density of the graphite was certainly very small but the uncertainty in the effective density, including voids in the column, may have been more significant. The total volume of the voids in the column amounted to only 0.3

per cent of the total volume. However, along a line through the detectors, about 5 cm of the total distance of about 96 cm, from the source to the last foil, consisted of voids. These voids were mainly due to the crescent shaped spaces between the fuel port plugs and the tips of the fuel ports. The absolute effect of these voids was difficult to determine but a consideration of the source of the slowing down density far out indicated that the voids could have resulted in a larger relative increase in the activity of the foils far from the source and, thus, could have contributed to the shape of the original ln Ar^2 versus r distribution.

In the determination of the experimental age, the graphite column was assumed to be infinite. Davis (4) determined the width of a column which would give an error of less than 1 per cent in the measured age for fission neutrons in graphite, to be approximately 43 inches. No such determination was made for the height of the pile, which was assumed to be infinite in the determinations for the width. Although the required size of the column would be greater for Pu-Be neutrons than fission neutrons, a consideration of the size of the column used in this study indicates that it should be large enough in both length and width for the infinite assumption to be valid.

CONCLUSIONS AND RECOMMENDATIONS

Due to the large statistical uncertainty in the measured activity, the apparent deviation from the theoretically indi-

cated distribution and the strong dependance of the age on the distribution, all far from the source, the results of the experimental portion of this study were not conclusive.

The age for the Pu-Be source as determined experimentally was about 10 per cent higher than the values previously reported (1), (2) for the experimental ages for Ra-α-Be and Po-Be sources; and it agreed very well with the age as calculated, both in this study and previously (2), for the Ra-α-Be and Po-Be sources, using the experimental spectra; and it was about 4 per cent higher than the age as calculated using the calculated Pu-Be spectrum. These comparisons, along with the consideration of a strong possibility of an error in the experimentally determined spectra, indicated that the age as determined experimentally in this study was probably at least 4 per cent high.

The age as calculated theoretically appeared to agree quite well with the calculated ages previously reported for similar sources. A comparison of the monoenergetic ages obtained in the calculation of the fission age, with the monenergetic ages as determined by more rigorous methods, would give a better indication as to the error involved in the Fermi age approximation as corrected by the first and last collisions. Although the error in the age for high energy neutron sources, using the Fermi age approximation, is greater than that for low energy neutrons from the fission source, the amount of error assumed in this study should have been sufficient. Even if the error were somewhat larger than assumed in this study, the overall error would still

be small enough so that this method of calculation should give a reasonable answer.

The method used in this study to calculate the age, from a fission source to 1.44 ev in graphite, could also be used to calculate the age to 1.44 ev for various sources in various media, where the age approximations are reasonably valid.

The largest factor contributing to the error in the experimental determination of the age, was the low foil activity for foils far from the source. Any increase in the count rate, or decrease in the background activity, would greatly increase the reliability of the determination.

The possible effects of induced long life foil activity, residual foil activity and foil contamination, should be carefully investigated.

The effects on the measured distribution by the voids in the measuring region of the column should be studied by completely filling these voids with graphite.

Although the measurements indicated that the foil spacing was sufficient and that the amount of cadmium in the column at any one time was not excessive, a more detailed study of these effects would perhaps be warranted.

A possible method to check for a constant counting error in the determination of the measured distribution, and to more accurately determine the shape of the ln Ar^2 versus r curve far from the source, would be to perform identical experiments using both Pu-Be and Po-Be sources. The increased foil activity due

to the increased source strength of the Po-Be source, would allow a more realistic evaluation of the shape of the ln Ar^2 versus r curve and should lessen the effects of constant counting errors due to background.

ACKNOWLEDGMENT

The author wishes to take this opportunity to express his appreciation to those who have so generously given of their time and experience to make this study possible. In particular, the author wishes to express his sincere gratitude to:

Dr. William R. Kimel, Head of the Department of Nuclear Engineering, for his guidance in the course of this study and critical suggestions made regarding the composition of this paper.

Richard C. Bailie, who suggested the feasibility of the method of calculation employed in this study, for the generous contribution of his excellent experience and time in outlining the basic IBM-650 computer program and for his many suggestions and aids in experimental procedure.

The remainder of the Department of Nuclear Engineering staff and students, for their suggestions and support.

The author also wishes to express his gratitude to the Kansas State University Engineering Experiment Station, for their financial support and to the Atomic Energy Commission, who through their fellowship program and material support, have made the opportunity of this study possible.

LITERATURE CITED

1) Amaldi, E.
in, Handbuch der physik. Vol. 38, Part II, Springer, Berlin, 1959.

2) Bogart, D., J. P. Cusick and D. F. Shook.
Discrepencies between experimental and theoretical ages for Po-Be and Ra-Be neutrons in water. Suppl. Nuc. Sci. and Eng., 2, 1 (1959).

3) Cranberg, L., G. Frye, N. Nereson and L. Rosen.
Fission neutron spectrum of U-235. Phys. Rev., 103:662 (1956).

4) Davis, W. G.
The design of a slowing down experiment. A.E.R.E. R/M 96 (1956).

5) Faulkner, J. E.
Age measurements in LiF. CF-54-8-98, (1954).

6) Glasstone, S., and M. C. Edlund.
The elements of nuclear reactor theory. D. Van Nostrand, Princeton, (1952).

7) Hastings, Cecil.
Approximations for digital computers. Princeton Univ., Princeton, N. J., (1955).

8) Hill, J. E., L. D. Roberts and T. E. Fitch.
Slowing down distribution of U-235 fission neutrons from a point source in light water. AECD-3392, (1948).

9) Hill, J. E., L. D. Roberts and G. McCammon.
Slowing down of fission neutrons in graphite. AECD-3390, (1949).

10) Hess, W. N.
Neutrons from (α,n) sources. UCRL-3839, (1957).

11) Howerton, R. J.
Tabulated neutron cross sections. UCRL-5226, (1958).

12) Hughes, D. J.
Pile neutron research. Addison-Wesley: Cambridge, (1953).

13) Hughes, D. J., and R. B. Schwartz.
Neutron cross sections. Suppl. 1, BNL-325, 2nd ed., (1960).

14) Marshak, R. E.
Theory of the slowing down of neutrons by elastic collisions with atomic nuclei. Rev. Mod. Phys., 19:185, (1947).

15) Reactor physics constants. ANL-5800, (1958).

16) Stewart, L.
The energy spectrum of neutrons from a Pu-Be source. Phys. Rev., 98:740 (1955).

17) Valente, F. A., and R. E. Sullivan.
The age of Pu-Be neutrons in light water. Nuc. Sci. Eng., 6, 2 (1959).

18) Wade, J. W.
Neutron age in mixtures of D_2O and H_2O. Nuc. Sci. and Eng., 4, 12 (1958).

19) Weinberg, A. M., and E. P. Wigner.
Theory of neutron chain reactors. Univ. of Chicago, (1958).

20) Whitmore, B. G., and W. B. Baker.
The energy spectrum of neutrons from a Po-Be source. Phys. Rev., 78:799 (1950).

APPENDIX

Correction of Foil Activities for Finite Sizes of Sources and Detectors

A simplified source correction has been worked out (18) for various source and detector geometries, assuming the distribution to be Gaussian. By further assuming the source to be a flat rectangle with length and width equal to the length and diameter of the source, the difference in the actual and measured activities is given as

$$A(r_o) - A_m(r_o) = -\left(\frac{b_1^2 + b_2^2 + 24\, a_2^2}{24 r_o}\right)\left(\frac{dA}{dr}\right)_{r_o}$$

where b_1 and b_2 are the length and width, respectively, of the rectangular source, a_2 is the radius of the detection foil, $A(r_o)$ is the activity induced by a point source in a point detector at r_o, and r_o is the distance between the center of the source and the center of the foil. $A_m(r_o)$ is the measured activity of the finite foil at r_o. Since this correction is small, the derivative $(dA/dr)r_o$, can be taken to be the slope of the experimental curve, A_m versus r.

The geometry correction factor

$$k = \frac{A(r_o)}{A_m(r_o)}$$

is plotted in Fig. (3) as a function of the distance r, from the source, for the two source geometries used.

Description and Explanation of the IBM-650 Code used to Determine the Analytical Age

The computer code is basically written to solve for the age as given by Eq. (32), when the integrals in this equation are replaced by the solutions given in Eq.'s (12) or (14), depending on σ_0 being greater than or equal to zero. The program is written in Soap form and floating point. The Soap output is listed at the end of this section, and a logic diagram, outlining the various procedures and operations, is given in Plate VII.

The code is written such that the energies at which the cross section data is taken are arbitrary, except that the cross section, between any two data points, must be essentially a straight line function of energy. If the cross sections corresponding to the energy limits of an i_{th} fraction of neutrons are not in the stored data, the program will interpolate the required values, using a straight line interpolation.

In determining the value of τ_i and the contribution of $f_i \tau_i$, for the fraction of neutrons slowing down from $(\bar{E}_o)_i$ to $\bar{E}_i$, there are several possibilities which must be considered with regard to the cross section input data. For each i_{th} interval, the machine reads in a fraction data card and will then search through the cross section data until it finds an E_n' which is either greater than or equal to $\bar{E}_i$. The program will then proceed to calculate τ_i, and $f_i \tau_i$, for the interval, taking into account all of the possibilities outlined in the logic diagram for the cross section data in the interval $\bar{E}_i$ to $(\bar{E}_o)_i$, and will

interpolate to obtain the cross sections at the end points when necessary. The possibility of dividing by zero, or the square of a very small number, as the case may be in Eq. (12), for σ_o equal to zero, or a very small number, is avoided by using Eq. (14), when σ_o is very small or zero. The criteria for using Eq. (14) is that σ_o must be less than 0.001. As all of the σ's are greater than one, or nearly equal to one, this criteria results in very little error with respect to the accuracy with which the cross sections are actually known.

The cross sections, and the energies corresponding to the cross sections, are punched on one per card load cards. The cross sections are loaded into drum locations 0 to 750 and the corresponding energies are loaded into drum locations 750 to 1500. For each cross section stored, a corresponding energy must also be stored such that the cross sections and the corresponding energies are in the same relative location in relation to the first cross section and the first energy in each storage group. The cross section, as a function of energy, must be placed in the storage locations in a sequence of increasing energy, with the cross section corresponding to the lowest energy being placed in the first location. The energy corresponding to the first piece of cross section data must be less than or equal to the lowest energy limit for any of the i_{th} energy groups.

The neutron fractions, f_i, and the corresponding average source energies, $\bar{E}_i$, and average fission energies, $(\bar{E}_o)_i$, are punched on regular 80 by 80 cards with $\bar{E}_i$, $(\bar{E}_o)_i$ and f_i being

the first, second and third words, respectively. These cards are placed in the program deck immediately following a blank card placed at the end of the cross section data. The cards containing the neutron fraction data are read into the computer, one at a time, according to the program instructions. These cards must be in order, with the lowest energy card being first. The sequence of card input is then; first, program deck; second, cross sections and corresponding energies; third, blank card; and fourth, neutron fraction data.

When calculating the fission age, from fission energy to resonance energy, the second term in the first collision correction, as given in Eq. (32), can be eliminated by changing the instruction address of instruction number 1974 from 1725 to 1825.

Table 13 lists the symbols which are used to represent the constants used in the program, along with the definitions of the symbols and the corresponding drum locations.

The symbols used in the program, corresponding to the various terms in Eq.'s (12), (14) and (32) are:

KP = K'

KPP = K''

EI = $(\bar{E})_i$

EF = $(\bar{E}_o)_i$

E indexed by A = E'_n, indicated by SIGMA-A in the logic diagram

SIGMI = σ_s $(\bar{E})_i$

SIGMF = σ_s $(\bar{E}_o)_i$

SIGMO = $\sigma_o (E')_n$

SIGMA indexed by A = $(E')_n$, indicated by SIGMA-A in the logic diagram

SUM

$$= \sum_{i=1}^{I} \left[\int_{\bar{E}_i}^{E_1'} \frac{1}{\sigma_s^{\,2}(E)} \frac{dE}{E} + \int_{E_2'}^{E_3'} \frac{1}{\sigma_s^{\,2}(E)} \frac{dE}{E} + \cdots \int_{E_m'}^{(\bar{E}_o)_i} \frac{1}{\sigma_s^{\,2}(E)} \frac{dE}{E} \right]$$

SLOPE = m

TAUE = Age between the energy limits of the i_{th} energy intervals, not including the first collision effect

TAUEP = TAUE plus the first collision effect between the energy limits of the i_{th} energy interval

TAU = Summation of the TAUE, weighted by the fractions, f_i, for all of the energy intervals previously calculated

TAUP = Summation of the TAUEP plus the first collision effect, weighted by the fractions, f_i, for all of the energy intervals previously calculated

FR = Fraction of neutrons in i_{th} energy interval

FRTOT = Total fraction of neutrons for which the age has been calculated.

The program is designed to give eight answers for each of the i_{th} energy interval calculations. The answers are punched, eight words per card, at the completion of the calculation for each i_{th} energy group. The answers, in the order in which they appear in the columns of the print-out and as previously defined, are EI, EF, FRTOT, SUM, TAUE, TAU, and TAUP.

The natural logarithm sub-routine used in the program, was one of the approximations given by Hastings (8) and was found to

Table 8. Definitions and drum locations for the symbols representing the constants used in the computer program.

Symbol :	Definition	:Drum location
A	Atomic weight	1550
RHO	Density	1600
MU	Average cosine of the scattering angle	1650
PSI	Logarithmic energy decrement	1700
NA	Avogadro's number	1750
THREE	Three	1800
ONE	One	1850
ZERO	Zero	1900
FOUR	Four	1950
TWO	Two	1501
PRECN	Criteria placed on the minimum magnitude of σ_0 for which Eq. (14) can be used	1551

give very accurate results over the entire range of logarithms used in the calculations.

The total running time for the program was approximately 45 minutes.

EXPLANATION OF PLATE VII

Logic diagram for the IBM-650 computer program

PLATE VII

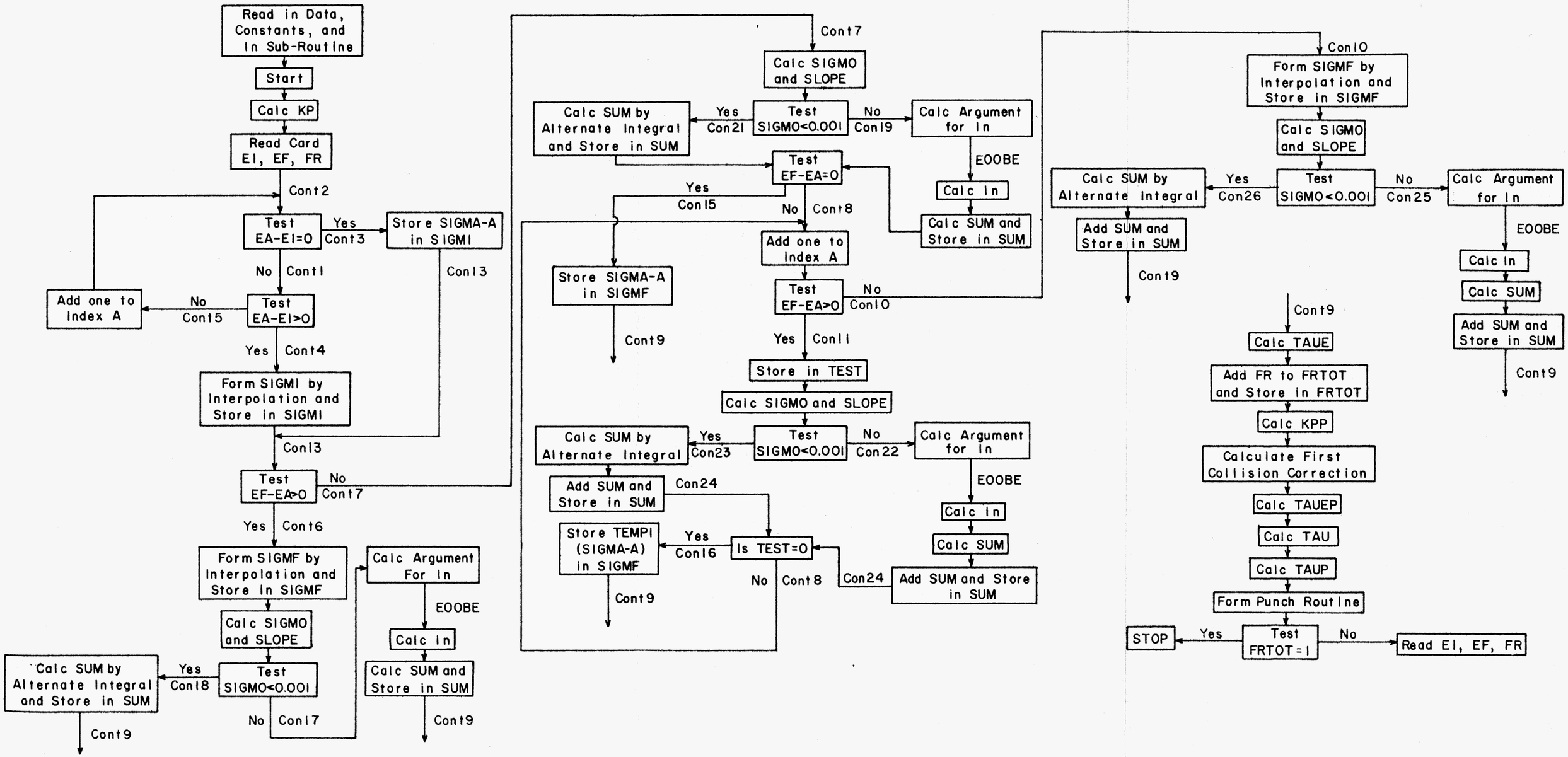
Read in Data, Constants, and In Sub-Routine
Start
Calc KP
Read Card EI, EF, FR
Cont2
Test EA-EI=0
Yes
Cont3
Store SIGMA-A in SIGMI
Con13
No
Cont1
Add one to Index A
No
Cont5
Test EA-EI>0
Yes
Cont4
Form SIGMI by Interpolation and Store in SIGMI
Con13
Test EF-EA>0
No
Cont7
Yes
Cont6
Form SIGMF by Interpolation and Store in SIGMF
Calc SIGMO and SLOPE
Test SIGMO<0.001
Yes
Con18
Calc SUM by Alternate Integral and Store in SUM
Cont9
No
Con17
Calc Argument For In
EOOBE
Calc In
Calc SUM and Store in SUM
Cont9
Cont7
Calc SIGMO and SLOPE
Test SIGMO<0.001
Yes
Con21
Calc SUM by Alternate Integral and Store in SUM
No
Con19
Calc Argument for In
EOOBE
Calc In
Calc SUM and Store in SUM
Test EF-EA=0
Yes
Con15
No
Cont8
Store SIGMA-A in SIGMF
Cont9
Add one to Index A
Test EF-EA>0
No
Con10
Yes
Con11
Store in TEST
Calc SIGMO and SLOPE
Test SIGMO<0.001
Yes
Con23
Calc SUM by Alternate Integral
Add SUM and Store in SUM
Con24
No
Con22
Calc Argument for In
EOOBE
Calc In
Calc SUM
Add SUM and Store in SUM
Con24
Store TEMPI (SIGMA-A) in SIGMF
Cont9
Yes
Con16
Is TEST=0
No
Cont8
Con10
Form SIGMF by Interpolation and Store in SIGMF
Calc SIGMO and SLOPE
Test SIGMO<0.001
Yes
Con26
Calc SUM by Alternate Integral
Add SUM and Store in SUM
Cont9
No
Con25
Calc Argument for In
EOOBE
Calc In
Calc SUM
Add SUM and Store in SUM
Cont9
Cont9
Calc TAUE
Add FR to FRTOT and Store in FRTOT
Calc KPP
Calculate First Collision Correction
Calc TAUEP
Calc TAU
Calc TAUP
Form Punch Routine
STOP
Yes
Test FRTOT=1
No
Read EI, EF, FR

Soap

Output

for

The

IBM-650 Computer Program

used in the Age Calculations

```
                BLR   9999          1500
                BLR   1977          1986        PRINT
                BLR   1951          1960        READ
                SYN   EI            1951
                SYN   EF            1952
                SYN   FR            1953
                SYN   SIGMA         0000
                SYN   E             0750
                SYN   START         1999
A                12    0000          0052      ATOMIC WT
RHO              16    0000          0051      DENSITY
MU               55    5100          0049      AVG S COS
PSI              15    8000          0050      LN E DECR
NA               60    2470          0050      AVAG NO
THREE            30    0000          0051
ONE              10    0000          0051
ZERO             00    0000          0000
FOUR             00    0000          0051
TWO              20    0000          0051
PRECN            10    0000          0048
EOOBP   STD      NEXT                          LN SUB
        LDD                 EOOBE
        FMP      TENB       NEXT
TENB             43    4294          4850
EOOBE   STD      EXIT
        STU      ARGU
        NZE                 HALT
        BMI      HALT
        RAU      ARGU
        STL      FACT
        FSB      ONEF
        BMI      SETD       SETU
SETD    RAU      ARGU
        FSB      ONEF
        BMI                 INTE
        FAD      ONEF
        FMP      TWOF
        STU      ARGU
        RAU      FACT
        FSB      TEMPP
        STU      FACT       SETD
SETU    RAU      ARGU
        FSB      TWOF
        BMI      SUBR
        FAD      TWOF
        FDV      TWOF
        STU      ARGU
        RAU      FACT
        FAD      TEMPP
        STU      FACT       SETU
SUBR    FAD      ONEF       INTE
INTE    STU      ARGU
        NZU      SPIN       JUMP
SPIN    RAU      ASEV
        FMP      ARGU
        FAD      ASIX
        FMP      ARGU
        FAD      AFIV
        FMP      ARGU
        FAD      AFOU
        FMP      ARGU
        FAD      ATHR
        FMP      ARGU
        FAD      ATWO
        FMP      ARGU
        FAD      AONE
        FMP      ARGU       JUMP
JUMP    FAD      FACT       EXIT
ONEF             10    0000          0051
TWOF             20    0000          0051
TEMPP            69    3147          1850
HALT             01    1234        EXIT
ASEV             10    7573          6949
ASIX    -        55    1199          5949
AFIV             13    4639          2750
AFOU    -        22    5873          2850
ATHR             32    8233          1250
ATWO    -        49    9470          1550
AONE             99    9981          0350
START   LDD      ZERO
        STD      TAU                           SET TAU
        STD      TAUP                          TAUP AND
        STD      FRTOT                         FRACT TO O
        RAU      ONE
        FSB      MU                            FORM KP
        STU      TEMP
        RAU      A
        FMP      A
        FDV      THREE
        FDV      NA
        FDV      NA
        FDV      TEMP
        FDV      RHO
        FDV      RHO
        FDV      PSI
        STU      KP         READ
READ    RCD       1951                         KP  READ
        RAA       0000      CONT2              FR EF EI
CONT2   RAU      E          A
        FSB      EI
        NZU      CONT1      CONT3
CONT1   BMI      CONT5      CONT4
CONT5   AXA       0001      CONT2
CONT4   STU      NUM                           FORM SIGMI
        LDD      E          A                  BY INTERPO
        STD      DEN                           LATION
        SXA       0001
        RSU      E          A
        FAD      DEN
        STU      DEN
        RAU      NUM
        FDV      DEN
        STU      TEMP
```

```
  1    0000    00
  2    0000    00
  3    0000    00
  4    0000    00
  5    0000    00
  6    0000    00
  7    0000    00
  8    0000    00
  9    0000    00
 10    1550    12  0000  0052
 11    1600    16  0000  0051
 12    1650    55  5100  0049
 13    1700    15  8000  0050
 14    1750    60  2470  0050
 15    1800    30  0000  0051
 16    1850    10  0000  0051
 17    1900    00  0000  0000
 18    1950    00  0000  0051
 19    1501    20  0000  0051
 20    1551    10  0000  0048
 21    1601    24  1504  1507
 22    1507    69  1510  1513
 23    1510    39  1563  1504
 24    1563    43  4294  4850
 25    1513    24  1516  1519
 26    1519    21  1524  1527
 27    1527    45  1530  1531
 28    1530    46  1531  1534
 29    1534    60  1524  1529
 30    1529    20  1533  1536
 31    1536    33  1539  1515
 32    1515    46  1518  1569
 33    1518    60  1524  1579
 34    1579    33  1539  1565
 35    1565    46  1568  1619
 36    1568    32  1539  1615
 37    1615    39  1618  1668
 38    1668    21  1524  1577
 39    1577    60  1533  1537
 40    1537    33  1540  1517
 41    1517    21  1533  1518
 42    1569    60  1524  1629
 43    1629    33  1618  1545
 44    1545    46  1548  1549
 45    1549    32  1618  1595
 46    1595    34  1618  1718
 47    1718    21  1524  1627
 48    1627    60  1533  1587
 49    1587    32  1540  1567
 50    1567    21  1533  1569
 51    1548    32  1539  1619
 52    1619    21  1524  1677
 53    1677    44  1581  1532
 54    1581    60  1584  1589
 55    1589    39  1524  1574
 56    1574    32  1727  1503
 57    1503    39  1524  1624
 58    1624    32  1777  1553
 59    1553    39  1524  1674
 60    1674    32  1827  1603
 61    1603    39  1524  1724
 62    1724    32  1877  1653
 63    1653    39  1524  1774
 64    1774    32  1927  1703
 65    1703    39  1524  1824
 66    1824    32  1528  1505
 67    1505    39  1524  1532
 68    1532    32  1533  1516
 69    1539    10  0000  0051
 70    1618    20  0000  0051
 71    1540    69  3147  1850
 72    1531    01  1234  1516
 73    1584    10  7573  6949
 74    1727    55  1199  5949
 75    1777    13  4639  2750
 76    1827    22  5873  2850
 77    1877    32  8233  1250
 78    1927    49  9470  1550
 79    1528    99  9981  0350
 80    1999    69  1900  1753
 81    1753    24  1506  1509
 82    1509    24  1512  1665
 83    1665    24  1768  1521
 84    1521    60  1850  1555
 85    1555    33  1650  1578
 86    1578    21  1582  1535
 87    1535    60  1550  1605
 88    1605    39  1550  1651
 89    1651    34  1800  1701
 90    1701    34  1750  1751
 91    1751    34  1750  1801
 92    1801    34  1582  1632
 93    1632    34  1600  1851
 94    1851    34  1600  1901
 95    1901    34  1700  1502
 96    1502    21  1556  1559
 97    1559    70  1951  1552
 98    1552    80  0000  1508
 99    1508    60  2750  1655
100    1655    33  1951  1628
101    1628    44  1631  1682
102    1631    46  1634  1585
103    1634    50  0001  1508
104    1585    21  1590  1543
105    1543    69  2750  1803
106    1803    24  1606  1609
107    1609    51  0001  1715
108    1715    61  2750  1705
109    1705    32  1606  1583
110    1583    21  1606  1659
111    1659    60  1590  1645
112    1645    34  1606  1656
113    1656    21  1582  1635
```

```
                RSU  SIGMA  A                                  114   1635    61 2000  1755
                STU  TEMP1                                      115   1755    21 1560  1613
                AXA   0001                                      116   1613    50 0001  1669
                RAU  SIGMA  A                                   117   1669    60 2000  1805
                FAD  TEMP1                                      118   1805    32 1560  1637
                FMP  TEMP                                       119   1637    39 1582  1732
                FSB  SIGMA  A                                   120   1732    33 2000  1678
                RSU   8003                                      121   1678    61 8003  1685
                STU  SIGMI                 SIGMI                122   1685    21 1640  1593
                SXA   0001    CON13                             123   1593    51 0001  1599
CON13           LDD  ZERO                                       124   1599    69 1900  1853
                STD  SUM                                        125   1853    24 1706  1709
                AXA   0001                                      126   1709    50 0001  1765
                LDD   8005                                      127   1765    69 8005  1571
                STD  AIN                   STORE  IRA           128   1571    24 1874  1728
                RAU  EF                    INITIAL              129   1728    60 1952  1557
                FSB  E        A                                 130   1557    33 2750  1778
                BMI  CONT6    CONT7                             131   1778    46 1681  1782
CONT7           RAU  E        A            FORM  INTE           132   1782    60 2750  1855
                FSB  EI                    GRAL  FOR            133   1855    33 1951  1828
                STU  TEMP                  1ST  INTER           134   1828    21 1582  1735
                RAU  SIGMA  A              VAL  EF  MIN         135   1735    60 2000  1905
                FSB  SIGMI                 US  EA  O  OR        136   1905    33 1640  1617
                FDV  TEMP                  POS                  137   1617    34 1582  1832
                STU  SLOPE                                      138   1832    21 1586  1639
                RSU  EI                                         139   1639    61 1951  1756
                FMP  SLOPE                                      140   1756    39 1586  1636
                FAD  SIGMI                                      141   1636    32 1640  1667
                STU  SIGMO                                      142   1667    21 1522  1525
                RAL  PRECN                                      143   1525    65 1551  1806
                SML  SIGMO                                      144   1806    18 1522  1878
                BMI  CON19    CON21                             145   1878    46 1731  1882
CON19           RSU  ONE                                        146   1731    61 1850  1856
                FDV  SIGMI                                      147   1856    34 1640  1690
                STU  TEMP                                       148   1690    21 1582  1785
                RAU  ONE                                        149   1785    60 1850  1906
                FDV  SIGMA  A                                   150   1906    34 2000  1602
                FAD  TEMP                                       151   1602    32 1582  1759
                FDV  SIGMO                                      152   1759    34 1522  1572
                STU  TEMP                                       153   1572    21 1582  1835
                RAU  E        A                                 154   1835    60 2750  1607
                FMP  SIGMI                                      155   1607    39 1640  1740
                FDV  EI                                         156   1740    34 1951  1652
                FDV  SIGMA  A                                   157   1652    34 2000  1702
                LDD           E00BE        GO  TO  LN           158   1702    69 1657  1513
                STU  LNX2                  SUB  ROUTIN          159   1657    21 1582  1815
                FDV  SIGMO                                      160   1815    34 1522  1622
                FDV  SIGMO                                      161   1622    34 1522  1672
                FAD  TEMP                                       162   1672    32 1582  1809
                STU  SUM                                        163   1809    21 1706  1859
                RAU  EF                                         164   1859    60 1952  1707
                FSB  E        A                                 165   1707    33 2750  1928
                NZU  CONT8    CON15                             166   1928    44 1781  1932
CON21           RSU  ONE                   ALTERNATE            167   1882    61 1850  1757
                FDV  E        A            INTEGRAL             168   1757    34 2750  1752
                FDV  E        A                                 169   1752    34 2750  1802
                STU  TEMP                                       170   1802    21 1582  1885
                RAU  ONE                                        171   1885    60 1850  1807
                FDV  EI                                         172   1807    34 1951  1852
                FDV  EI                                         173   1852    34 1951  1902
                FAD  TEMP                                       174   1902    32 1582  1909
                FDV  TWO                                        175   1909    34 1501  1903
                FDV  SLOPE                                      176   1903    34 1586  1686
                FDV  SLOPE                                      177   1686    34 1586  1736
                STU  SUM                   SUM  FOR             178   1736    21 1706  1610
                RAU  EF                    CONT7                179   1610    60 1952  1857
                FSB  E        A                                 180   1857    33 2750  1679
                NZU  CONT8    CON15                             181   1679    44 1781  1932
CON15           LDD  SIGMA  A              SIGMF  FOR           182   1932    69 2000  1554
                STD  SIGMF    CONT9        FIRST                183   1554    24 1907  1660
CONT8           AXA   0001                                      184   1781    50 0001  1687
                RAU  EF                                         185   1687    60 1952  1558
                FSB  E        A                                 186   1558    33 2750  1729
                BMI  CON10    CON11                             187   1729    46 1633  1683
CON11           STU  TEST                                       188   1683    21 1538  1541
                LOD  E        A            FORM  INTEG          189   1541    69 2750  1604
                STD  TEMP                  RAL  FOR  IN         190   1604    24 1582  1935
                LDD  SIGMA  A              TERMEDIATE           191   1935    69 2000  1654
                STD  TEMP1                 INTERVALS            192   1654    24 1560  1663
                SXA   0001            E    F  MINUS            193   1663    51 0001  1719
                RAU  TEMP                  EA  O  OR            194   1719    60 1582  1737
                FSB  E        A            POS                  195   1737    33 2750  1779
                STU  TEMP2                                      196   1779    21 1684  1787
                RAU  TEMP1                                      197   1787    60 1560  1865
                FSB  SIGMA  A                                   198   1865    33 2000  1829
                FDV  TEMP2                                      199   1829    34 1684  1734
                STU  SLOPE                                      200   1734    21 1586  1689
                RSU  E        A                                 201   1689    61 2750  1608
                FMP  SLOPE                                      202   1608    39 1586  1786
                FAD  SIGMA  A                                   203   1786    32 2000  1879
                STU  SIGMO                                      204   1879    21 1522  1575
                RAL  PRECN                                      205   1575    65 1551  1658
                SML  SIGMO                                      206   1658    18 1522  1929
                BMI  CON22    CON23                             207   1929    46 1733  1783
CON22           RSU  ONE                                        208   1733    61 1850  1708
                FDV  SIGMA  A                                   209   1708    34 2000  1704
                STU  TEMP2                                      210   1704    21 1684  1837
                RAU  ONE                                        211   1837    60 1850  1758
                FDV  TEMP1                                      212   1758    34 1560  1710
                FAD  TEMP2                                      213   1710    32 1684  1511
                FDV  SIGMO                                      214   1511    34 1522  1722
                STU  TEMP2                                      215   1722    21 1684  1887
                RAU  TEMP                                       216   1887    60 1582  1937
                FMP  SIGMA  A                                   217   1937    39 2000  1754
                FDV  E        A                                 218   1754    34 2750  1804
                FDV  TEMP1                                      219   1804    34 1560  1760
                LDD           E00BE        GO  TO  LN           220   1760    69 1713  1513
                STU  LNX3                  SUB  ROUTIN          221   1713    21 1818  1621
                FDV  SIGMO                                      222   1621    34 1522  1772
                FDV  SIGMO                                      223   1772    34 1522  1822
                FAD  TEMP2                                      224   1822    32 1684  1561
                FAD  SUM                                        225   1561    32 1706  1833
                STU  SUM      CON24                             226   1833    21 1706  1810
CON23           RSU  ONE                   ALTERNATE            227   1783    61 1850  1808
                FDV  TEMP                  INTEGRAL             228   1808    34 1582  1883
                FDV  TEMP                                       229   1883    34 1582  1933
                STU  TEMP2                                      230   1933    21 1684  1987
                RAU  ONE                                        231   1987    60 1850  1858
                FDV  E        A                                 232   1858    34 2750  1854
                FDV  E        A                                 233   1854    34 2750  1904
                FAD  TEMP2                                      234   1904    32 1684  1611
                FDV  TWO                                        235   1611    34 1501  1908
                FDV  SLOPE                                      236   1908    34 1586  1836
                FDV  SLOPE                 SUM  FOR             237   1836    34 1586  1886
                FAD  SUM                   CONT11               238   1886    32 1706  1784
                STU  SUM      CON24                             239   1784    21 1706  1810
CON24           AXA   0001                                      240   1810    50 0001  1566
                RAU  TEST                                       241   1566    60 1538  1643
                NZU  CONT8    CON16                             242   1643    44 1781  1598
CON16           LDD  TEMP1                 SIGMAF  FOR          243   1598    69 1560  1763
                STD  SIGMF    CONT9        FIRST                244   1763    24 1907  1660
CON10           SXA   0001                 FORM  SIGMF          245   1633    51 0001  1739
```

```
        RAU  E       A          BY INTERPO  246   1759    60 2750 1960
        STU  TEMP               LATION      247   1660    21 1582 1936
        RAU  SIGMA   A                      248   1936    60 2000 1910
        STU  TEMP1                          249   1910    21 1560 1813
        AXA   0001                          250   1813    50 0001 1769
        RAU  E       A                      251   1769    60 2750 1661
        FSB  TEMP                           252   1661    33 1582 1711
        STU  TEMP                           253   1711    21 1582 1588
        RAU  E       A                      254   1588    60 2750 1761
        FSB  EF                             255   1761    33 1952 1580
        FDV  TEMP                           256   1580    34 1582 1834
        STU  TEMP                           257   1834    21 1582 1638
        RAU  SIGMA   A                      258   1638    60 2000 1811
        FSB  TEMP1                          259   1811    33 1560 1688
        FMP  TEMP                           260   1688    39 1582 1884
        FSB  SIGMA   A                      261   1884    33 2000 1630
        RSU   8003                          262   1630    61 8003 1738
        STU  SIGMF              SIGMF       263   1738    21 1907 1861
        SXA   0001              FORM INTE   264   1861    51 0001 1717
        RAU  EF                 GRAL FOR    265   1717    60 1952 1911
        FSB  E       A          LAST INTER  266   1911    33 2750 1680
        STU  TEMP               VAL EF LES  267   1680    21 1582 1788
        RAU  SIGMF              EA NEG      268   1788    60 1907 1961
        FSB  SIGMA   A                      269   1961    33 2000 1730
        FDV  TEMP                           270   1730    34 1582 1934
        STU  SLOPE                          271   1934    21 1586 1789
        RSU  E       A                      272   1789    61 2750 1612
        FMP  SLOPE                          273   1612    39 1586 1838
        FAD  SIGMA   A                      274   1838    32 2000 1780
        STU  SIGMO                          275   1780    21 1522 1625
        RAL  PRECN                          276   1625    65 1551 1662
        SML  SIGMO                          277   1662    18 1522 1830
        BMI  CON25      CON26               278   1830    46 1888 1938
CON25   RSU  ONE                            279   1888    61 1850 1712
        FDV  SIGMA   A                      280   1712    34 2000 1762
        STU  TEMP                           281   1762    21 1582 1988
        RAU  ONE                            282   1988    60 1850 1812
        FDV  SIGMF                          283   1812    34 1907 1862
        FAD  TEMP                           284   1862    32 1582 1912
        FDV  SIGMO                          285   1912    34 1522 1872
        STU  TEMP                           286   1872    21 1582 1839
        RAU  EF                             287   1839    60 1952 1962
        FMP  SIGMA   A                      288   1962    39 2000 1863
        FDV  E       A                      289   1863    34 2750 1913
        FDV  SIGMF                          290   1913    34 1907 1963
        LDD             E00BE   GO TO LN    291   1963    69 1616 1513
        STU  LNX4               SUBROUTINE  292   1616    21 1520 1523
        FDV  SIGMO                          293   1523    34 1522 1922
        FDV  SIGMO                          294   1922    34 1522 1972
        FAD  TEMP                           295   1972    32 1582 1514
        FAD  SUM                            296   1514    32 1706 1889
        STU  SUM        CONT9               297   1889    21 1706 1660
CON26   RSU  ONE                ATERNATE    298   1938    61 1850 1564
        FDV  EF                 INTEGRAL    299   1564    34 1952 1614
        FDV  EF                             300   1614    34 1952 1664
        STU  TEMP                           301   1664    21 1582 1939
        RAU  ONE                            302   1939    60 1850 1714
        FDV  E       A                      303   1714    34 2750 1764
        FDV  E       A                      304   1764    34 2750 1814
        FAD  TEMP                           305   1814    32 1582 1864
        FDV  TWO                            306   1864    34 1501 1914
        FDV  SLOPE                          307   1914    34 1586 1989
        FDV  SLOPE              SUMM FOR    308   1989    34 1586 1790
        FAD  SUM                CON10       309   1790    32 1706 1840
        STU  SUM        CONT9               310   1840    21 1706 1660
CONT3   LDD  SIGMA   A                      311   1682    69 2000 1964
        STD  SIGMI      CON13               312   1964    24 1640 1599
CONT6   RAU  E       A          FORM SIGMF  313   1681    60 2750 1915
        FSB  EF                 FOR SINGLE  314   1915    33 1952 1880
        STU  TEMP               INTERVAL    315   1880    21 1582 1890
        LDD  E       A                      316   1890    69 2750 1965
        STD  TEMP1                          317   1965    24 1560 1666
        SXA   0001                          318   1666    51 0001 1573
        RAU  TEMP1                          319   1573    60 1560 1716
        FSB  E       A                      320   1716    33 2750 1930
        STU  DEN                            321   1930    21 1606 1766
        RAU  TEMP                           322   1766    60 1582 1940
        FDV  DEN                            323   1940    34 1606 1816
        STU  TEMP                           324   1816    21 1582 1990
        LDD  SIGMA   A                      325   1990    69 2000 1866
        STD  TEMP1                          326   1866    24 1560 1916
        AXA   0001                          327   1916    50 0001 1623
        RAU  SIGMA   A                      328   1623    60 2000 1966
        FSB  TEMP1                          329   1966    33 1560 1591
        FMP  TEMP                           330   1591    39 1582 1641
        FSB  SIGMA   A                      331   1641    33 2000 1831
        RSU   8003                          332   1831    61 8003 1691
        STU  SIGMF              SIGMF       333   1691    21 1907 1767
        FSB  SIGMI              FORM INTE   334   1767    33 1640 1817
        STU  TEMP               GRAL FOR    335   1817    21 1582 1741
        RAU  EF                 SINGLE IN   336   1741    60 1952 1867
        FSB  EI                 TERVAL EF   337   1867    33 1951 1881
        STU  TEMP1              MINUS EA    338   1881    21 1560 1917
        RAU  TEMP               NEG         339   1917    60 1582 1791
        FDV  TEMP1                          340   1791    34 1560 1967
        STU  SLOPE                          341   1967    21 1586 1841
        RSU  EI                             342   1841    61 1951 1868
        FMP  SLOPE                          343   1868    39 1586 1891
        FAD  SIGMI                          344   1891    32 1640 1918
        STU  SIGMO                          345   1918    21 1522 1675
        RAL  PRECN                          346   1675    65 1551 1968
        SML  SIGMO                          347   1968    18 1522 1931
        BMI  CON17      CON18               348   1931    46 1941 1991
CON17   RSU  ONE                            349   1941    61 1850 1819
        FDV  SIGMI                          350   1819    34 1640 1542
        STU  TEMP                           351   1542    21 1582 1592
        RAU  ONE                            352   1592    60 1850 1869
        FDV  SIGMF                          353   1869    34 1907 1919
        FAD  TEMP                           354   1919    32 1582 1969
        FDV  SIGMO                          355   1969    34 1522 1673
        STU  TEMP                           356   1673    21 1582 1642
        RAU  EF                             357   1642    60 1952 1570
        FMP  SIGMI                          358   1570    39 1640 1692
        FDV  EI                             359   1692    34 1951 1620
        FDV  SIGMF                          360   1620    34 1907 1670
        LDD             E00BE   GOTO LN     361   1670    69 1723 1513
        STU  LNX1               SUB ROUTIN  362   1723    21 1742 1695
        FDV  SIGMO                          363   1695    34 1522 1773
        FDV  SIGMO                          364   1773    34 1522 1823
        FAD  TEMP                           365   1823    32 1582 1720
        STU  SUM        CONT9               366   1720    21 1706 1660
CON18   RSU  ONE                ALTERNATE   367   1991    61 1850 1770
        FDV  EF                 INTEGRAL    368   1770    34 1952 1820
        FDV  EF                             369   1820    34 1952 1870
        STU  TEMP                           370   1870    21 1582 1792
        RAU  ONE                            371   1792    60 1850 1920
        FDV  EI                             372   1920    34 1951 1970
        FDV  EI                             373   1970    34 1951 1671
        FAD  TEMP                           374   1671    32 1582 1721
        FDV  TWO                            375   1721    34 1501 1771
        FDV  SLOPE                          376   1771    34 1586 1842
        FDV  SLOPE              SUM FOR     377   1842    34 1586 1892
```

```
                STU  SUM        CONT9       CONT6           378    1892     21  1706  1660
CONT9           RAU  SUM                                    379    1660     60  1706  1821
                FMP  KP                                     380    1821     39  1556  1871
                STU  TAUE                                   381    1871     21  1526  1942
                RAU  FR                     FORM  KPP       382    1942     60  1953  1921
                FAD  FRTOT                                  383    1921     32  1768  1745
                STU  FRTOT                                  384    1745     21  1768  1971
                RAU  ONE                                    385    1971     60  1850  1873
                FSB  MU                                     386    1873     33  1650  1992
                FMP  KP                                     387    1992     39  1556  1923
                FMP  PSI                                    388    1923     39  1700  1973
                STU  KPP                    KPP             389    1973     21  1693  1546
                RAU  ONE                    FORM  FIRST     390    1546     60  1850  1924
                FDV  SIGMF                  COLLISION       391    1924     34  1907  1974
                FDV  SIGMF                  CORRECTION      392    1974     34  1907  1725
                STU  TEMP                                   393    1725     21  1582  1743
                RSU  ONE                                    394    1743     61  1850  1775
                FDV  SIGMI                                  395    1775     34  1640  1793
                FDV  SIGMI                                  396    1793     34  1640  1843
                FAD  TEMP                                   397    1843     32  1582  1825
                FMP  KPP                                    398    1825     39  1693  1893
                STU  FIRST                                  399    1893     21  1648  1875
                RAU  TAUE                                   400    1875     60  1526  1943
                FAD  FIRST                                  401    1943     32  1648  1925
                STU  TAUEP                                  402    1925     21  1993  1596
                RAU  TAUE                                   403    1596     60  1526  1544
                FMP  FR                                     404    1544     39  1953  1975
                FAD  TAU                                    405    1975     32  1506  1594
                STU  TAU                                    406    1594     21  1506  1576
                RAU  TAUEP                                  407    1576     60  1993  1547
                FMP  FR                                     408    1547     39  1953  1626
                FAD  TAUP                                   409    1626     32  1512  1644
                STU  TAUP                                   410    1644     21  1512  1676
                LOD  EI                                     411    1676     69  1951  1726
                STD   1977                                  412    1726     24  1977  1694
                LOD  EF                                     413    1694     69  1952  1776
                STD   1978                                  414    1776     24  1978  1744
                LOD  FRTOT                                  415    1744     69  1768  1826
                STD   1979                                  416    1826     24  1979  1794
                LOD  SUM                                    417    1794     69  1706  1876
                STD   1980                                  418    1876     24  1980  1844
                LOD  TAUE                                   419    1844     69  1526  1894
                STD   1981                                  420    1894     24  1981  1944
                LOD  TAUEP                                  421    1944     69  1993  1646
                STD   1982                                  422    1646     24  1982  1994
                LOD  TAU                                    423    1994     69  1506  1926
                STD   1983                                  424    1926     24  1983  1795
                LOD  TAUP                                   425    1795     69  1512  1976
                STD   1984                                  426    1976     24  1984  1845
                PCH   1977                                  427    1845     71  1977  1895
                RAU  FRTOT                                  428    1895     60  1768  1945
                FSB  ONE                                    429    1945     33  1850  1995
                NZU  READ       STOP                        430    1995     44  1559  1696
```

Tables and Graphs

Table 9. Summary of the neutron fraction data, used in the age calculations, for the Pu-Be and the Po-Be sources.

Fraction of total neutrons f_i	Cumulative fraction of total neutrons	Average energy, $\bar{E}_i$ Experimental Pu-Be	Calculated Pu-Be	Experimental Po-Be
0.01	0.01	0.07	0.28	0.09
0.01	0.02	0.21	0.48	0.27
0.01	0.03	0.33	0.60	0.40
0.01	0.04	0.44	0.68	0.50
0.01	0.05	0.52	0.76	0.56
0.01	0.06	0.61	0.83	0.63
0.01	0.07	0.70	0.89	0.70
0.01	0.08	0.79	0.95	0.78
0.01	0.09	0.83	1.01	0.87
0.01	0.10	0.98	1.06	0.99
0.01	0.11	1.07	1.12	1.11
0.01	0.12	1.16	1.17	1.22
0.01	0.13	1.26	1.23	1.34
0.01	0.14	1.36	1.28	1.45
0.01	0.15	1.46	1.34	1.56
0.01	0.16	1.56	1.40	1.66
0.01	0.17	1.66	1.45	1.77
0.01	0.18	1.77	1.51	1.82
0.01	0.19	1.83	1.57	1.97
0.01	0.20	2.00	1.63	2.06
0.01	0.21	2.10	1.70	2.14
0.01	0.22	2.21	1.76	2.22
0.01	0.23	2.31	1.82	2.30
0.01	0.24	2.41	1.90	2.37
0.01	0.25	2.50	1.98	2.44
0.01	0.26	2.58	2.12	2.51
0.01	0.27	2.61	2.30	2.57
0.01	0.28	2.74	2.42	2.64
0.01	0.29	2.80	2.52	2.70
0.01	0.30	2.83	2.60	2.76
0.01	0.31	2.95	2.68	2.84
0.01	0.32	3.01	2.75	2.89
0.01	0.33	3.09	2.81	2.94
0.01	0.34	3.16	2.87	3.00
0.01	0.35	3.22	2.93	3.06
0.01	0.36	3.29	2.98	3.12
0.01	0.37	3.35	3.04	3.18
0.01	0.38	3.41	3.09	3.24
0.01	0.39	3.48	3.14	3.29
0.01	0.40	3.54	3.19	3.35
0.01	0.41	3.60	3.24	3.41
0.01	0.42	3.66	3.29	3.46

Table 9 (cont.)

Fraction of total neutrons f_i	Cumulative fraction of total neutrons	Average energy, $\bar{E}_i$ Experimental Pu-Be	Calculated Pu-Be	Experimental Po-Be
0.01	0.43	3.73	3.34	3.53
0.01	0.44	3.79	3.38	3.60
0.01	0.45	3.85	3.42	3.66
0.01	0.46	3.90	3.47	3.75
0.01	0.47	3.96	3.51	3.82
0.01	0.48	4.02	3.56	3.89
0.01	0.49	4.08	3.60	3.97
0.01	0.50	4.15	3.65	4.05
0.01	0.51	4.20	3.70	4.12
0.01	0.52	4.26	3.74	4.20
0.01	0.53	4.33	3.79	4.26
0.01	0.54	4.40	3.83	4.34
0.01	0.55	4.46	3.88	4.40
0.01	0.56	4.52	3.92	4.47
0.01	0.57	4.60	3.96	4.54
0.01	0.58	4.66	4.01	4.60
0.01	0.59	4.72	4.06	4.66
0.01	0.60	4.80	4.11	4.72
0.01	0.61	4.86	4.16	4.78
0.01	0.62	4.94	4.21	4.84
0.01	0.63	5.01	4.26	4.90
0.01	0.64	5.10	4.31	4.96
0.01	0.65	5.18	4.37	5.01
0.01	0.66	5.26	4.42	5.07
0.01	0.67	5.36	4.48	5.14
0.01	0.68	5.47	4.54	5.20
0.01	0.69	5.57	4.60	5.28
0.01	0.70	5.68	4.66	5.36
0.01	0.71	5.80	4.72	5.44
0.01	0.72	5.91	4.80	5.52
0.01	0.73	6.01	4.87	5.61
0.01	0.74	6.12	4.96	5.70
0.01	0.75	6.24	5.06	5.78
0.01	0.76	6.34	5.17	5.87
0.01	0.77	6.45	5.30	5.97
0.01	0.78	6.55	5.46	6.01
0.01	0.79	6.65	5.72	6.15
0.01	0.80	6.75	6.07	6.26
0.01	0.81	6.85	6.33	6.37
0.01	0.82	6.95	6.51	6.49
0.01	0.83	7.05	6.67	6.60
0.01	0.84	7.15	6.83	6.72
0.01	0.85	7.25	6.97	6.85
0.01	0.86	7.35	7.10	6.97
0.01	0.87	7.48	7.24	7.10

Table 9 (concl.)

Fraction of total neutrons f_i	Cumulative fraction of total neutrons	Average energy, $\bar{E}_i$ Experimental Pu-Be	Calculated Pu-Be	Experimental Po-Be
0.01	0.88	7.56	7.36	7.22
0.01	0.89	7.67	7.50	7.34
0.01	0.90	7.77	7.65	7.47
0.01	0.91	7.84	7.78	7.59
0.01	0.92	8.00	7.93	7.72
0.01	0.93	8.15	8.10	7.85
0.01	0.94	8.31	8.25	8.00
0.01	0.95	8.55	8.42	8.15
0.005	0.955	8.77	8.57	8.30
0.005	0.960	8.95	8.66	8.40
0.005	0.965	9.11	8.77	8.55
0.005	0.970	9.25	8.87	8.70
0.005	0.975	9.40	9.01	8.92
0.005	0.980	9.54	9.15	9.17
0.005	0.985	9.68	9.31	9.50
0.005	0.990	9.83	9.51	9.78
0.005	0.995	10.00	9.75	10.05
0.005	1.000	10.25	10.15	10.40

Table 10. Summary of the neutron fraction data used to calculate the fission neutron age, and the calculated monoenergetic ages, with and without the first collision correction, from the average energy of each neutron fraction interval, to 1.44 ev.

Fraction of total neutrons f_i	Cumulative fraction of total neutrons	Average energy $\bar{E}_i$	Age from $\bar{E}_i$ to 1.44 ev. Without correction	Age from $\bar{E}_i$ to 1.44 ev. With correction
0.01	0.01	0.03	156.15	158.64
0.01	0.02	0.10	176.55	179.12
0.01	0.03	0.15	183.64	186.30
0.01	0.04	0.19	188.00	190.87
0.01	0.05	0.24	192.66	195.73
0.01	0.06	0.26	194.33	197.49
0.01	0.07	0.30	197.45	200.80
0.01	0.08	0.33	199.63	203.14
0.01	0.09	0.35	201.04	204.65
0.01	0.10	0.38	203.07	206.85
0.01	0.11	0.42	205.68	209.68
0.01	0.12	0.45	207.57	211.76
0.01	0.13	0.47	208.81	213.13
0.01	0.14	0.50	210.64	215.16
0.01	0.15	0.53	212.44	217.12
0.01	0.16	0.56	214.20	219.07
0.01	0.17	0.59	215.94	221.01
0.01	0.18	0.62	217.65	222.91
0.01	0.19	0.65	219.34	224.77
0.01	0.20	0.68	221.01	226.63
0.01	0.21	0.71	222.66	228.46
0.01	0.22	0.74	224.30	230.27
0.01	0.23	0.76	225.38	231.47
0.01	0.24	0.77	226.98	233.28
0.01	0.25	0.81	228.05	234.47
0.01	0.26	0.85	230.16	236.82
0.01	0.27	0.87	231.21	237.99
0.01	0.28	0.90	232.77	239.75
0.01	0.29	0.93	234.33	241.50
0.01	0.30	0.95	235.36	242.66
0.01	0.31	0.98	236.90	244.40
0.01	0.32	1.01	238.44	246.15
0.01	0.33	1.04	239.97	247.92
0.01	0.34	1.07	241.51	249.69
0.01	0.35	1.10	243.05	251.47
0.01	0.36	1.13	244.59	253.25
0.01	0.37	1.16	246.13	255.05
0.01	0.38	1.19	247.68	256.86
0.01	0.39	1.22	249.23	258.67
0.01	0.40	1.25	250.79	260.47

Table 10 (cont.)

Fraction of total neutrons f_i	Cumulative fraction of total neutrons	Average energy $\bar{E}_i$	Age from $\bar{E}_i$ to 1.44 ev. Without correction	Age from $\bar{E}_i$ to 1.44 ev. With correction
0.01	0.41	1.29	252.87	262.89
0.01	0.42	1.32	254.43	264.73
0.01	0.43	1.35	256.04	266.58
0.01	0.44	1.38	257.58	268.45
0.01	0.45	1.41	259.17	270.32
0.01	0.46	1.45	261.29	272.79
0.01	0.47	1.48	262.89	274.65
0.01	0.48	1.51	264.49	276.52
0.01	0.49	1.55	266.63	279.04
0.01	0.50	1.59	268.78	281.59
0.01	0.51	1.62	270.41	283.56
0.01	0.52	1.65	272.05	285.56
0.01	0.53	1.69	274.26	288.28
0.01	0.54	1.72	275.93	290.27
0.01	0.55	1.76	278.17	292.88
0.01	0.56	1.80	280.41	295.50
0.01	0.57	1.84	282.66	298.15
0.01	0.58	1.88	284.93	300.94
0.01	0.59	1.91	286.65	303.26
0.01	0.60	1.96	289.66	307.84
0.01	0.61	2.00	292.21	311.65
0.01	0.62	2.05	295.45	313.32
0.01	0.63	2.09	296.76	310.89
0.01	0.64	2.13	298.89	316.77
0.01	0.65	2.17	301.19	320.16
0.01	0.66	2.22	304.17	324.14
0.01	0.67	2.26	306.57	326.73
0.01	0.68	2.31	309.54	329.93
0.01	0.69	2.36	312.49	333.28
0.01	0.70	2.41	315.45	336.67
0.01	0.71	2.47	318.96	340.12
0.01	0.72	2.52	321.77	342.37
0.01	0.73	2.57	324.45	344.58
0.01	0.74	2.63	327.54	347.19
0.01	0.75	2.69	330.39	348.47
0.01	0.76	2.75	332.92	349.15
0.01	0.77	2.81	335.09	348.77
0.01	0.78	2.88	337.10	347.65
0.01	0.79	2.95	338.45	343.82
0.01	0.80	3.02	341.31	377.18
0.01	0.81	3.10	347.44	373.79
0.01	0.82	3.18	351.03	368.22
0.01	0.83	3.26	353.54	366.90

Table 10 (concl.)

Fraction of total neutrons f_i	Cumulative fraction of total neutrons	Average energy $\bar{E}_i$	Age from $\bar{E}_i$ to 1.44 ev. Without correction	Age from $\bar{E}_i$ to 1.44 ev. With correction
0.01	0.84	3.35	355.74	366.79
0.01	0.85	3.44	357.58	367.46
0.01	0.86	3.54	359.43	369.12
0.01	0.87	3.65	361.35	370.64
0.01	0.88	3.75	363.29	374.69
0.01	0.89	3.87	365.77	378.06
0.01	0.90	4.00	368.72	383.42
0.01	0.91	4.14	372.29	387.94
0.01	0.92	4.30	375.83	388.12
0.01	0.93	4.47	379.58	397.99
0.01	0.94	4.67	386.46	414.80
0.01	0.95	4.89	395.87	427.01
0.005	0.955	5.10	404.62	443.68
0.005	0.960	5.25	412.38	451.44
0.005	0.965	5.42	419.75	442.71
0.005	0.970	5.60	427.83	472.95
0.005	0.975	5.83	441.24	490.03
0.005	0.980	6.08	454.23	497.87
0.005	0.985	6.43	465.08	511.93
0.005	0.990	6.90	497.82	564.52
0.005	0.995	7.60	522.82	558.69
0.005	1.000	9.00	556.74	597.92

Table 11. Total microscopic neutron cross sections used in the age calculations. The cross section at 1.44 ev was taken to be 4.7 barns.

Energy E_n', Mev	Cross section (E_n') barns	Energy E_n', Mev	Cross section (E_n') barns	Energy E_n', Mev	Cross section (E_n') barns
0.015	4.70	2.080	3.40	4.30	2.05
0.020	4.65	2.083	2.70	4.35	2.00
0.030	4.55	2.084	2.50	4.40	1.90
0.075	4.50	2.085	2.10	4.44	1.75
0.10	4.48	2.093	1.80	4.50	1.60
0.13	4.45	2.13	1.70	4.55	1.50
0.15	4.40	2.17	1.65	4.60	1.45
0.17	4.33	2.21	1.61	4.63	1.40
0.20	4.20	2.32	1.59	4.67	1.35
0.22	4.15	2.44	1.55	4.75	1.30
0.24	4.10	2.56	1.60	4.80	1.29
0.31	3.90	2.62	1.61	4.85	1.28
0.36	3.75	2.69	1.69	4.90	1.29
0.40	3.65	2.76	1.80	4.92	1.33
0.45	3.51	2.83	2.00	4.93	1.43
0.50	3.38	2.87	2.15	4.95	1.64
0.54	3.30	2.90	2.34	4.96	1.60
0.60	3.17	2.92	2.50	5.01	1.20
0.70	3.00	2.94	2.80	5.10	1.15
0.80	2.85	2.95	3.10	5.16	1.14
0.90	2.72	2.96	3.00	5.20	1.12
1.00	2.60	2.97	2.80	5.25	1.15
1.08	2.50	2.98	2.00	5.30	1.10
1.20	2.36	2.99	1.60	5.32	1.10
1.30	2.26	3.00	1.30	5.35	1.15
1.40	2.16	3.04	1.10	5.37	1.40
1.50	2.08	3.06	1.20	5.40	1.64
1.60	2.00	3.12	1.50	5.42	1.50
1.70	1.91	3.17	1.70	5.45	1.20
1.80	1.85	3.20	1.80	5.48	1.15
1.85	1.82	3.29	2.05	5.50	1.15
1.90	1.78	3.37	2.20	5.55	1.20
1.95	1.70	3.40	2.25	5.60	1.07
2.00	1.63	3.50	2.34	5.65	1.02
2.02	1.60	3.55	2.30	5.70	1.00
2.03	1.60	3.64	2.40	5.80	1.02
2.05	1.70	3.70	2.15	5.90	1.05
2.06	1.90	3.82	2.10	6.00	1.07
2.068	2.40	3.87	2.05	6.05	1.07
2.071	2.70	3.92	2.00	6.10	1.10
2.073	3.80	3.98	1.90	6.15	1.15
2.074	4.60	4.02	1.85	6.20	1.25
2.075	4.80	4.12	1.80	6.23	1.50
2.076	5.00	4.18	1.85	6.25	1.75
2.078	4.30	4.23	1.95	6.26	2.15
2.079	4.00	4.25	2.00	6.27	2.45

Table 11 (concl.)

Energy E_n', Mev	Cross section (E_n') barns	Energy E_n', Mev	Cross section (E_n') barns
6.28	2.60	8.00	1.80
6.30	2.50	8.05	1.75
6.32	2.00	8.10	1.80
6.35	1.50	8.20	1.85
6.38	1.20	8.22	1.80
6.40	1.10	8.24	1.70
6.43	1.05	8.28	1.35
6.48	1.00	8.30	1.25
6.50	0.95	8.33	1.15
6.55	0.75	8.35	1.10
6.60	0.60	8.40	1.05
6.62	0.67	8.45	1.05
6.65	0.90	8.50	1.05
6.67	0.95	8.60	1.08
6.70	1.00	8.70	1.10
6.80	0.95	8.80	1.11
6.90	0.88	8.90	1.12
7.00	0.80	9.00	1.12
7.05	0.75	9.40	1.13
7.10	0.85	9.60	1.14
7.15	1.35	10.00	1.15
7.18	1.55	10.80	1.20
7.20	1.65		
7.30	1.75		
7.35	1.78		
7.40	1.80		
7.45	1.77		
7.50	1.70		
7.53	1.60		
7.57	1.40		
7.59	1.25		
7.60	1.20		
7.62	1.35		
7.65	1.50		
7.70	1.61		
7.72	1.60		
7.74	1.55		
7.76	1.85		
7.77	2.00		
7.80	2.16		
7.82	2.00		
7.83	1.90		
7.85	1.85		
7.90	1.90		
7.95	1.85		

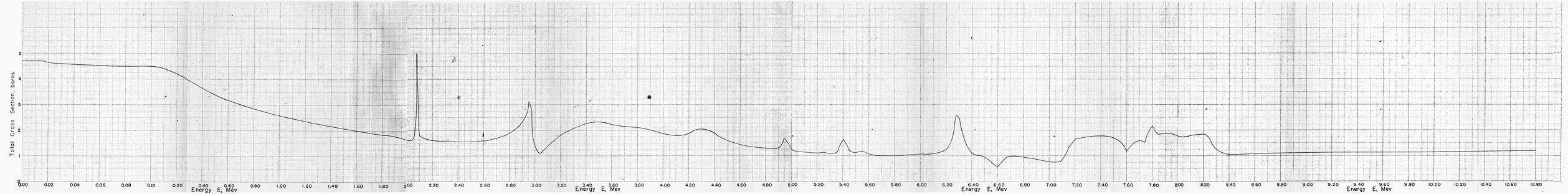

Fig. 12. Total neutron cross section for graphite.

THE EXPERIMENTAL DETERMINATION AND ANALYTICAL VERIFICATION OF THE AGE OF PU-BE SOURCE NEUTRONS IN GRAPHITE

by

CHARLES URBAN STEICHEN

B. S., Kansas State University, 1959

AN ABSTRACT OF A THESIS

submitted in partial fulfillment of the

requirements for the degree

MASTER OF SCIENCE

Department of Nuclear Engineering

KANSAS STATE UNIVERSITY
OF AGRICULTURE AND APPLIED SCIENCE

1960

The age of Pu-Be neutrons was measured in graphite and calculations were performed to theoretically predict the age from measured and calculated spectra.

The measured age was evaluated from the second moment of the slowing down distribution at the 1.44 ev resonance of indium. The measured value of the age was 416 cm^2, corrected to a graphite density of 1.60 gm/cm^3. This result, however, was not conclusive because of the large statistical uncertainty in the measured distribution due to low foil activity. Comparisons with the results obtained from previous calculations and experiments for similar sources, i.e., Ra-α-Be and Po-Be, indicate that the result was probably at least 4 per cent too high.

The theoretical calculations were performed using previously measured and calculated spectra and the Fermi age approximation, corrected for first and last collision effects. The ages were calculated from Pu-Be and from Po-Be source spectra to the fission source spectrum and these values were then added to the accepted value of the age, for the fission spectrum, to obtain the total age from source energies to indium resonance. The age of fission neutrons, to 1.44 ev, was also calculated in order to estimate the error in the procedure. The calculated age values, corrected for the first collision effect, were 298.4, 422.2, 403.5 and 416.4 cm^2 for the fission (also including the last collision correction), experimental Pu-Be, calculated Pu-Be and experimental Po-Be spectra, respectively. These values compared reasonably

well with previously determined values for similar spectra.

The calculations were carried out with the Kansas State University IBM-650 computer. A complete description of the computer program is also given.